Dry Carbonate Process for CO_2 capture and storage: Integration with solar thermal power

D. Bonaventura [a, b], R. Chacartegui [b, *], J. M. Valverde [c], J.A. Becerra [b], C. Ortiz [c], J. Lizana [d]

[a] Politecnico di Torino, Corso Duca degli Abruzzi, 24, 10129 Torino, Italy
[b] Departamento de Ingeniería Energética, Universidad de Sevilla, Camino de los Descubrimientos s/n, 41092 Seville, Spain
[c] Facultad de Física, Universidad de Sevilla, Avda. Reina Mercedes s/n, 41012 Seville, Spain
[d] Departamento de Construcciones Arquitectónicas, Universidad de Sevilla, Avda. Reina Mercedes 2, 41012, Seville, Spain

* Corresponding author. Tel.: +34 954487243. E-mail address: ricardoch@us.es

Abstract

Capture and sequestration of CO_2 released by conventional fossil fuel combustion is an urgent need to mitigate global warming. In this work, main CO_2 capture and sequestration (CCS) systems are reviewed, with the focus on their integration with renewables in order to achieve power plants with nearly zero CO_2 emissions. As a case study, the manuscript analyses the integration of a CO_2 sorption-desorption cycle based on Na_2CO_3/$NaHCO_3$ into a coal fired power plant (CFPP) for CO_2 capture with solar support for sorbent regeneration. The Dry Carbonate Process relies on the use of a dry regenerable sorbent such as sodium carbonate (Na_2CO_3) to remove CO_2 from flue gases. Na_2CO_3 is converted to sodium bicarbonate ($NaHCO_3$) through reaction with CO_2 and water steam. Na_2CO_3 is regenerated when $NaHCO_3$ is heated, which yields a gas stream mostly containing CO_2 and H_2O. Condensation of H_2O produces a pure CO_2 stream suitable for its subsequent use or compression and sequestration. In this paper, the application of the Dry Carbonate CO_2 capture process in a coal-based power plant is studied with the goal of optimizing CO_2 capture efficiency, heat and power requirements. Integration of this CO_2 capture process requires an additional heat supply which would reduce the global power plant efficiency by around 9-10%. Dry Carbonate Process has the advantage compared with other CCS technologies that requires a relatively low temperature for sorbent regeneration (<200ºC). It allows an effective integration of medium temperature solar thermal power to assist $NaHCO_3$ decarbonation. This integration reduces efficiency losses to the associated with mechanical parasitic consumption, resulting in a fossil fuel energy penalty of 3-4% (including CO_2 compression). The paper shows the viability of the concept through economic analyses under different scenarios. The results suggest the interest of advancing in this Solar-CCS integrated concept, which shows favourable outputs compared to other CCS technologies.

Keywords

Carbon capture, Post-combustion carbon capture, Coal fired power plant, Dry Carbonate Process, CCS Economy, Solar thermal power.

Nomenclature

ASU: Air separation unit BAC: Biomass annual cost BFB: Bubbling fluidized bed CaL: Calcium-Looping process CCS: Carbon capture and storage CFB: Circulating fluidized bed CFPP: Coal-fired power plant COE: Cost of electricity c_{CO2}: Carbon tax COP21: 2015 Paris Climate Conference CPU: CO2 purification unit CSP: Concentrated solar power ECCS: Emission ratio with dry carbonate process integrated ECO2 AVOIDED: Avoided cost due to the avoided emission of CO2, EDRYCARBONATE: Carbon capture system installation cost ENET, GAIN, year: Annual benefit due to avoided emissions. EO&M: Operation and maintenance cost EINCR: Revenues due to electricity incremented cost Eref: Reference plant emission ratio ESOLAR: Solar plant installation cost ETOT, REV: Total annual revenues ETOT: Total investment cost FB: Fluidized Bed FC: Fuel cost FCF: Fixed charge factor FGD: Flue gas desulfurization GHG: Greenhouse gases IPCC: Intergovernmental Panel on Climate Change IRR: Internal rate of return (%)	$m_{CO2,\ FGPLANT}$: CO_2 mass flows of flue gas exits the CFPP $m_{CO2,\ CARB.OUT}$: CO_2 mass flows of flue gas exits the carbonator MEA: Monoethanolamine solvent NGCC: Natural gas combined cycles NPV: Net Present Value O&M: Operation and maintenance PCC: Post-combustion capture $P_{NET,\ year}$: Total electric energy per year produced by the plant. Q_{CFPP}: CFPP thermal power consumptions Q_{DC}: Dry carbonate thermal power consumption SE-SMR: Sorption-enhanced steam methane reforming SMR: Steam methane reforming SPB: Simple payback SPECCA: Specific energy consumption for CO_2 avoided TCR: Capital cost $ton_{CO2,\ ref:}$ Reference plant CO_2 emissions $ton_{CO2,\ CCS:}$ CO_2 emissions with the dry carbonate process integrated VOM: Variable cost $W_{CFPP:}$ CFPP net power production W_{COMP}: Electric consumption for CO_2 compression $W_{cons,\ DC:}$ Dry carbonate electric power consumption W_{solid}: Electric consumption for solids conveying WGS: Water gas shift YR: Yearly Revenues ε_{ABS}: Absorption efficiency η_{plant}: Plant efficiency η_{CCS}: Plant efficiency with the dry carbonate process integrated

1. Introduction

There is a worldwide interest in finding competitive solutions for capturing and sequestering the carbon dioxide (CO_2) released from fossil fuel combustion processes to mitigate global warming. In the 2015 Paris Climate Conference (COP21), a universal agreement signed by the consensus of 195 countries was reached, which has been ratified in 2016, to drastically reduce CO_2 emissions in order to keep global warming below 2°C from preindustrial levels [1]. To this end future coal-fired power plants (CFPPs) must be near to CO_2 emissions free. Currently, 76.5% of the electricity generation in the world is produced by non-renewable sources [2]. The main R&D challenge for the viability of CFPPs and other fossil fuel based facilities is to capture CO_2 by means of feasible and affordable technologies while, at the same time, penalties on power production and efficiency are minimized.

Carbon capture and storage (CCS) technologies can be classified into three main groups: pre-combustion, post-combustion and oxy-fuel combustion processes [3]. Despite post-combustion capture (PCC) processes are being widely investigated in the last years, Boundary Dam (100MWe) in Canada is currently the only commercial CFPP that applies CCS by using a chemical absorption process based on monoethanolamine (MEA). In amine-based systems the CO_2 loaded solvent is separated from the rest of the exhaust gas and heated, which yields relatively pure CO_2 ready for compression and sequestration. After regeneration, the solvent is cooled to be reused [4]. A main issue of systems based on amine absorption is the large amount of heat required to regenerate the solvent. This heat, which is usually obtained from the steam cycle, penalizes significantly the power plant efficiency. Moreover, amine-based systems have serious problems related to toxicity and corrosion [5]. In addition, additional power is required to compress the captured CO_2 for transporting it through the pipeline network to the storage site.

Among the new generation of CCS technologies under R&D the Dry Carbonate Process stands as one of the most interesting options. This process uses Na_2CO_3 solid particles as dry sorbent to separate CO_2 from other flue gases through the gas-solid carbonation reaction. An important advantage of this approach is that sorption can occur at relatively low temperature (below 100ºC) to achieve a high capture capacity whereas regeneration is also carried out at relatively low temperatures (around 200ºC). Such temperatures do not cause significant degradation of the sorbent besides of not requiring high amounts of energy supply [6]. Other advantages of the Dry Carbonate Process are the low cost of the sorbent as well as the high CO_2 sorption capacity [7]. Due to the high interest attracted by this technology, CO_2 capture pilot plants have been integrated in CFPP in USA and Korea [8]. Recent studies have analysed also its potential integration with the production of chemical products [9].

In this paper, a novel integration of the Dry Carbonate Process for CO_2 capture with solar thermal power is analysed. The relative low temperature in the regeneration reactor allows for an effective integration with solar thermal power, which supplies medium temperature heat at relatively reduced cost. This combination yields a significantly reduced penalty in the global efficiency compared with other technologies. Therefore, the Dry Carbonate Process has the potential for a real breakthrough as CO_2 capture system integrated in CFPP with a reduced penalty on the global process and a high CO_2 capture efficiency, which would help achieving a near to zero CO_2 emissions power plant. The deployment of the Dry Carbonate process could represent an enormous step forward to efficiently

retrofit power plants based on no-renewable fossil fuels. Such ambitious goal is fully aligned with both the IPCC projections (CCS should contribute by about 55% to the cumulative global mitigation effort until 2100 [10]) and the IEA roadmap (1000 GW of installed Concentrated Solar power capacity by 2050 [11]).

The present paper has the following structure. Firstly, an overview of CO_2 capture technologies is given. Different alternatives are discussed, highlighting advantages and challenges of the Dry Carbonate Process as compared to other techniques. Secondly, a case study based on the integration of a CFPP with the Dry Carbonate Process is described (layout, processes and chemistry). Based on these analyses an economic study is carried out to assess the proposed plant viability and sensitivity to different relevant parameters (price of electricity, cost of technologies, fuel cost variability, energy penalty, carbon taxes). The results obtained suggest the high interest of the proposed integration under some particular scenarios.

2. CO_2 capture technologies. A brief review

This section is devoted to an overview of the state of art regarding CO_2 capture technologies. It is structured around the three main CCS technologies (Figure 1), namely pre-combustion, post-combustion and oxy-fuel combustion processes [3].

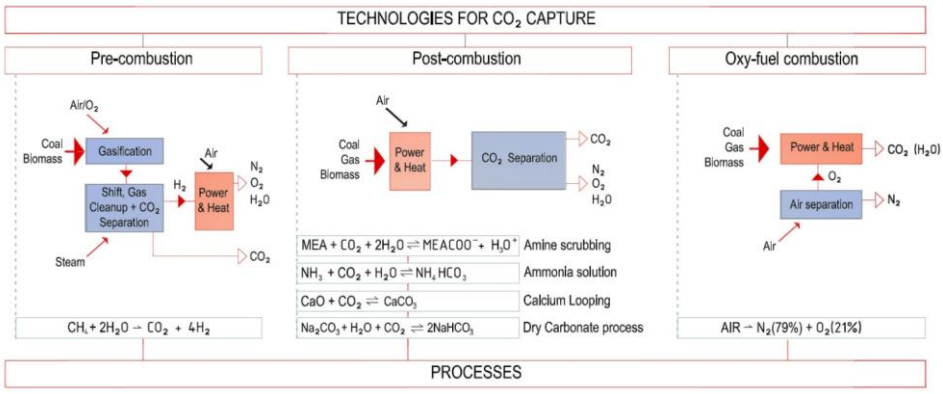

Figure 1: Overview of technologies for CO_2 capture.

2.1 Pre-combustion CO_2 capture

Pre-combustion CO_2 capture is based on the reaction of a fuel with oxygen or air with or without the presence of steam to produce a gaseous fuel, synthesis gas or syngas, which mainly consists of hydrogen and carbon monoxide. Carbon monoxide reacts afterwards with steam in a catalytic reactor (or shift converter) to produce CO_2 and more hydrogen. Finally, CO_2 is separated by means of physical or chemical absorption processes to obtain a hydrogen-rich fuel [10].

Syngas is usually generated from coal, biomass or natural gas by adding steam to the fuel (steam reforming) or by fuel partial oxidation. When natural gas is used as primary fuel in the conventional steam methane reforming (SMR) method the main reaction takes place in reformer tubes filled with catalyst [12]. In the case coal or biomass are used as fuel, gasification is the main conversion technology used to produce syngas. After syngas production, the water gas shift (WGS) reaction (Eq.1), involves the reaction between CO and steam to yield CO_2 and H_2 as products.

$$CO_{(g)} + H_2O_{(g)} \leftrightarrows CO_{2(g)} + H_2 \qquad \Delta H_{298K} = -41\frac{kJ}{mol} \qquad (1)$$

The high pressure (15-40 bar) of the produced gas stream (with a CO_2 content in the range of 15-60% in dry basis) facilitates the removal of CO_2 [13]. The captured CO_2 is ready to be compressed and stored whereas the rich H_2-product can be used for power production through a gas turbine [14], combined cycles [15] or in fuel cells [16].

The main advantage of pre-combustion capture is the production of CO_2 at elevated pressure, which reduces energy consumption for compression, and the production of a carbon-free fuel [10]. According to the IEA GHG program [17], an efficiency penalty of 16% is expected for natural gas combined cycles (NGCC) with pre-combustion CO_2 capture. This efficiency drop is caused by syngas production (6%), H_2/CO_2 separation (5%), the WGS process (3%), and CO_2 compression (2%) [12].

Due to the expected efficiency drop, current research is focussed on reducing energy losses and investment costs associated with CO_2 capture equipment. The most promising solution under study is based on the combination of reforming and the WGS reactions with CO_2 removal in one single stage, which shifts the reaction equilibrium towards the production of hydrogen. Thus, several H_2/CO_2 separation technologies have emerged in the last years based on membranes and solid sorbents [12]. In this regard, an modification of this process is the sorption-enhanced steam methane reforming (SE-SMR), where the process is enhanced by using a CO_2 sorbent in the reactor, which promotes the WGS reaction and achieves in situ CO_2 separation [18].

An option widely investigated in recent years is to integrate pre-combustion and post-combustion technologies, which allows exploiting potential synergies between both technologies [19]. Thus, SE-SMR-CaL and CaL enhanced gasification are being investigated. SE-SMR-CaL integration is based on CO_2 capture by CaO solids, which is thermodynamically favourable at the process conditions [20]. According to Martinez et al. [21], the SE-SMR-CaL integration achieves much higher H_2 production efficiencies (above 77%) in comparison with a conventional steam methane reforming (SMR) based plant using commercially available amines for CO_2 capture.

In the case of solid fuel gasification, it is also interesting to integrate the CaL process for increasing the hydrogen content in the syngas. According to Ramkumar and Fan thermodynamic analysis [22], the addition of CaO as sorbent allows to attain a hydrogen purity over 99% in the absence of a water-gas shift catalyst at near-stoichiometric steam to carbon (S:C) ratios, especially when operating at high pressures (>21 atm) [22].

2.2 Oxy-fuel combustion

In oxy-fuel combustion a fuel is burned using pure oxygen rather than air as the primary oxidant. As a result fuel consumption is diminished and flame temperature is higher as compared to air combustion, where part of the released heat is absorbed by nitrogen. Oxy-combustion requires an air separation process to remove nitrogen from the intake air to obtain an enriched oxygen stream with an oxygen concentration as high as 95%. To avoid a too high flame temperature by directly firing the fuel with pure oxygen, the mixture is diluted with CO_2 rich recycled flue gas, or staged combustion [23,24]. In this way combustion temperature and heat transfer rate are controlled, and conventional equipment designed for conventional fuel/air combustion can be used in the coal power plant retrofitting process [25]. According to Kather et al. [26] the flue gas recirculation appropriate to yield a mixture in the boiler with combustion temperatures and heat transfer fluxes similar to those obtained with conventional coal/air-combustion is in the range of 0.65-0.75 [27]. An alternative method to control flame temperature is the use of steam injection [28]. Although oxy-fuel combustion allows reducing CO_2 emissions quite efficiently, oxygen separation from air is a high energy demanding and costly process. Thus, the main drawback for the commercial deployment of oxy-combustion is the high energy consumption for pure O_2 production in the air separation unit (ASU). Cryogenic distillation is the common technique for this purpose, which requires an energy consumption of about 200 kWh per kg of pure O_2 [29,30].

After a purification process, the almost pure CO_2 stream (~95% vol) is suitable for compression and storage or utilization [31,32]. According to Escudero et al. [33], CO_2 purification unit (CPU) specific energy consumption can be estimated as 143 kWh/tCO_2. The energy penalty associated to the integration of oxy-fuel combustion is in the range 7–13% [26,33,34].

Oxy-combustion has been successfully demonstrated in large-scale pilot projects (30 MW_e) [27,35,36]. Currently, most of the research activities on oxy-combustion are focused on pulverized coal combustion. However, Fluidized Bed (FB) combustion seems to be also an interesting alternative technology for oxy-combustion [37]. FB oxy-combustion was employed in CIUDEN project [38] with a thermal power of 30MW_{th} obtained from burning diverse fuels (petroleum coke, subbituminous coal and biomass among others) in a Circulating Fluidized Bed (CFB) boiler. Oxy-combustion using bubbling fluidized beds (BFB) has been also tested at the pilot scale [39]. A detailed review on current and proposed large scale oxy-coal combustion demonstration projects is presented in [25].

2.3 Post-combustion CO_2 capture

Post-combustion capture refers to CO_2 removal from the exhaust gas of fossil fuel power plants, which can be accomplished by using chemical solvents, solid sorbents or electrochemical processes.

In the currently mature chemical absorption technology, the solvent (typically an amine solution such as MEA) binds chemically with the CO_2. Amine absorption and stripping consists of passing the post-combustion flue gas through an aqueous amine solvent, which absorbs CO_2 by chemical reaction [40]. Then, the solvent loaded with CO_2 (the "rich" solvent) is heated up above typically 120 °C in the regenerator reactor wherein the CO_2-amine chemical reaction is reversed to release nearly pure CO_2 and regenerate the amine. The so-called "lean" solvent is recycled back to the absorber to restart the

Comentado [U1]: ??

Comentado [U2]: Que unidades?, especificar

process while the released CO_2 is compressed to a suitable pressure for an efficient transportation and storage [41]. Amine-based PCC can efficiently remove around 90% of the CO_2 emissions.

In spite that CO_2 capture by chemical absorption using MEA is a well-established process in industry, the commercial deployment of this technology for post-combustion CO_2 capture at large scale is hindered by a combination of factors such as high energy penalty (8-12%) due to regeneration of the solvent [42,43], amine toxicity [44], solvent degradation [45] and equipment corrosion [46].

Sorption of CO_2 by solids (either by chemical reaction or physical adsorption) is an alternative method to chemical absorption with potential advantages linked to the arguably lower energy requirement for regeneration and easier operation and maintenance. Suitable sorbents for CO_2 removal should meet several requeirements including high sorption capacity, high selectivity towards CO_2, fast kinetics, mild conditions for desorption, and high multicycle stability [47].

The calcium looping (CaL) process [48] is at the basis of a 2nd generation PCC technology [47] that uses CaO, typically derived from natural limestone, to capture CO_2 from flue gases by means of the reversible carbonation/calcination reaction (Eq. 2):

$$CaO_{(s)} + CO_{2(g)} \leftrightarrows CaCO_{3(s)} \qquad \Delta H_{298K} = -178\frac{kJ}{mol} \qquad (2)$$

The sorbent is repeatedly cycled between two CFB reactors. In the carbonator, CO_2 from the flue gas is captured by carbonation of the CaO particles. Taking into account that flue gases exiting from CFPP generally contain a mole fraction of CO_2 in the range 10– 15% [48,49], carbonation proceeds at a satisfactory high rate at temperatures in the range 625–700°C while the reverse reaction to regenerate the sorbent is carried out in the calciner under high CO_2 partial pressure, thereby at much higher temperatures (900–950°C) in order to achieve complete decarbonation in a typically short residence time of a few minutes [50–53]. The regenerated CaO particles are returned to the carbonator while a concentrated stream of CO_2 is released from the calciner ready for compression, transport and sequestration. A drawback of the process is the progressive deactivation of the regenerated CaO with the number of cycles due to the harsh calcination conditions leading to marked grain sintering. Thus, the CaO residual conversion at these CaL conditions is just around 0.07-0.08 [54,55], which requires a periodic feed of fresh limestone (make-up) to replace the poorly active sorbent. The endothermicity of the calcination reaction and the temperature difference between sorbent streams entering and leaving the calciner make it necessary to provide a high-energy input to the calciner. In order to achieve the required calcination temperature without CO_2 dilution, Shimizu and co-workers [56] proposed to oxy-fire coal (auxiliary fuel) in the calciner with O_2 provided by an external air separation unit, whose estimated size would be approximately one third of that required for an oxy-fuel power plant. This option serves to reach the high temperatures in the calciner typical of oxy-firing while CO_2 is not diluted, albeit CaO deactivation is further enhanced by irreversible CaO sulphation and ashes due to in-situ coal oxycombustion [55–58]. Recently, a combination of Oxy-combustion and CaL technologies has been proposed for coal power plants with some expected benefits such as the reduction of the CaL system size [59].

The CaL technology has several potential advantages when compared to amine scrubbing including a higher CO_2 capture efficiency (above 90%) with minor energy penalty over the power plant (4-9%)

[19,60] and the low cost, wide availability and non-toxicity of natural CaO precursors such as natural limestone or dolomite [61]. Even though several pilot plant projects (~ 1-2 MW_{th}) are already showing promising results [52,62] the CaL technology has not yet reached a demonstration stage.

Another option for PCC is based on membrane separation, which uses the pressure difference between the flue gas and the removed CO_2. The membrane technology is generally useful to treat high-pressure gases [64,65] in spite of which a large number of researches have adapted it for post-combustion capture [43,66,67]. Regarding efficiency penalty associated to membranes use for PCC, it is estimated in the range of 4.9-8.5% [64]. Membrane separation is a promising solution to reduce the costs of PCC. However, the maximum pressure ratio attainable by feed compression and/or permeate vacuum is limited to approximately 10, due to cost and energy considerations [66].

A recently proposed option for PCC is the use of electrochemical processes in Molten Carbonate fuel cells. Some studies show that electricity generation in the fuel cell partially compensates the penalty on the original cycle in wastewater treatment plants [68] and power plants [69–71].

The development of dry CO_2 capture processes based on cheap materials operating at relatively low temperatures, which would require relatively low energy for sorbent regeneration, is considered as a promising pathway to advance in the deployment of CO_2 capture technologies [3,63]. In the present manuscript, the use of an abundant and cheap material such as sodium carbonate (Na_2CO_3) with a high dry CO_2 sorption capacity at relatively low temperatures is studied. Na_2CO_3 is the sorbent employed in the Dry Carbonate Process (DCP) early proposed in [72,73] and currently being demonstrated at the pilot-scale stage [74]. As Nelson et al. report [6], this capture process exhibits many potential advantages. First, sorbent regeneration is achieved at relatively low temperatures (100–200 °C) and it uses a dry sorbent. This helps decreasing considerably the energy required for sorbent regeneration as compared to amine based absorption, wherein much energy is lost due to the requirement of heating the large amounts of water in which the amine is dissolved. The DCP does not require any flue gas pretreatment and the reactor materials are not subjected to high thermal stresses or corrosive issues at the temperatures of operation. A further important advantage, as proposed in this work, is that dry sorbent regeneration in the range of working temperatures can be efficiently assisted by medium temperature solar thermal power, which significantly reduces energy penalty at affordable costs.

2.4 Challenges in the road to the deployment of CO_2 capture technologies

Each one of the above reviewed PCC technologies show specific advantages but also challenges to overcome at their different R&D development stages. Nonetheless, PCC is considered as the most appropriate technique to be applied in the short-term for its relatively easy integration in existing fossil fuel power plants [75]. PCC integration penalizes power plant performance and this hampers indirectly the global CO_2 emissions reduction. The use of renewable sources such as solar thermal energy or biomass to aid the process is a possibility for mitigating this penalty. An intense R&D activity is being carried out to assess the feasibility of PCC-solar integration with the focus on reducing solar installation costs and providing a significant fraction of the heat required for sorbent regeneration [76].

The main drawbacks that hinder the deployment of PCC technologies are the high cost of the full CCS chain and the high efficiency penalty imposed on the power plant. Further obstacles are the financing of CO_2 transport infrastructure, legal and regulatory frameworks and insurance for safe permanent CO_2 storage or utilization [63]. As discussed below, diverse alternatives have been analysed for mitigating the efficiency penalty through the assistance of solar thermal energy mainly focussed on amines and CaL based PCC systems. However, these studies fail generally to demonstrate net benefits from the solar-PCC integration in the absence of external incentives [77]. A main inconvenient for the integration of solar in the CaL process is that sorbent regeneration is rather energy intensive requiring calcination of large flow rates of solids at very high temperatures (900–950°C) [50]. On the other hand, sorbent regeneration in amine-based capture systems is carried out at relatively much lower temperatures (slightly above 120 ºC) [41]. Yet, regeneration of the aqueous amine solution involves heating a large amount of water which requires a high energy supply [78]. In this sense, the Dry Carbonate Process stands as a promising alternative since it demands a relatively small amount of energy supply for sorbent regeneration. In this process the dry sorbent (Na_2CO_3) is regenerated at much lower temperatures (150-200 ºC) as compared to the CaL system [6,72,74]. Thus, solar thermal energy requirements for sorbent regeneration would be significantly reduced, which would favour the flexibility and economic viability of the solar-PCC integration.

3. Integration of renewables on post-combustion carbon capture systems

A main objective of R&D activities on PCC is to significantly reduce CO_2 emissions from fossil fuel plants with a reduced penalty on the power plant efficiency due to the high amount of energy required by the CO_2 capture processes. One way on the road to facilitate demonstration and deployment of PCC technologies is the use of renewable energy sources such as solar or biomass. The energy supplied by these renewable sources does not contribute to additional CO_2 emissions and is thus CO_2 neutral in the global process.

The integration of solar thermal energy in PCC technologies can be achieved through two different strategies: i) by assisting sorbent regeneration, and ii) by contributing to power production to minimize the efficiency penalty. Main research activities regarding solar-assisted PCC are focused on amine-based CO_2 capture and the recently emerged CaL process. In order to mitigate the high penalty associated to amine-based capture systems, a number of R&D activities have been carried out to assess the use of solar thermal technologies:

- Parvareh et al. [76] analyzed the use of different solar thermal technologies to support amine-based PCC for retrofitting CFPPs. They concluded that the large amount of thermal energy required for solar integration in this PCC technology would need a huge thermal storage and considerably high solar capital costs, which raises doubts on the feasibility of solar integration in amine based CO_2 capture systems. In addition, the huge solar thermal energy requirement for such integration to be effective is not available in most geographical locations globally.
- Mokhtar et al. [79] reported a study to reduce the energy intensity of the CO_2 separation process for retrofitting existing fossil fuel power plants. Partial solar thermal energy integration was assessed to reduce the penalty derived from amine-based PCC energy input in a CFPP case study of 300MW_e. A main conclusion of this work is that the proposed

integration could be economically viable for solar collector costs of USD100/m^2 and if more than 22% of the required solvent regeneration energy is provided by solar thermal energy.

- A techno-economic analysis of solar-assisted PCC applied to different locations in Australia has been recently reported by Qadir et al. [77]. The application was divided into three subsystems: the power plant (660MW_e), the amine-based PCC plant and the solar collector field. Different solar technologies were compared under scenarios without and with heat integration between the three subsystems. Regarding solar collectors, the integration based on evacuated tube collectors performed better when heat integration between the three subsystems is properly acomplished, whereas parabolic trough collectors were more effective in the case without heat integration. The study concludes that process design (heat integration) and climatic constraints are important considerations for the effectiveness of solar-assisted PCC. However, the cases under study did not yield net benefits of using any of the solar collector technologies analyzed in the absence of incentives.
- Li et al. [80] studied the feasibility of integrating solar thermal energy into amine-based PCC for a 520MW_e CFPP. They concluded that, in order to achieve lower cost of electricity and cost of CO_2 avoidance as compared to the case without solar assisted PCC, the price of solar thermal collectors has to be lower than 150 USD/m^2 and 90 USD/m^2 for the solar trough and vacuum tube, respectively. Also, the viability of solar-assisted PCC was highly dependent on climate conditions.
- Cohen et al. [41] have reviewed the use of high temperature solar thermal technologies to assist amine-based PCC. As a main outcome, it is concluded that using high temperature solar thermal energy for direct electricity generation is more efficient than using solar energy for assisting sorbent regeneration.
- A small-scale pilot study has been carried out by Wang et al. [81,82] on amine-based PCC coupled with a solar thermal sub-system. Two types of solar collectors were used to gain the required thermal energy of the reboiler (parabolic trough collectors and linear Fresnel reflectors). Both of them could provide the required temperature heat source at the small-scale of the test. The results suggested that the efficiency of parabolic trough collectors was higher and less dependent on solar radiation.
- Carapellucci et al. [83] analyzed two options for integrating renewable energies into a CFPP with CO_2 post-combustion capture either using an auxiliary biomass boiler or a concentrating solar power (CSP) system. The obtained results for the biomass boiler integration showed that the power plant capacity was increased by approximately 14% whereas the energy penalty (-8%) was weakly reduced as compared to the reference case (with an efficiency of 42%). Regarding the CSP system it was shown that its integration yields a 14% lower than the reference case whereas the net efficiency decreased during the day to 31%.
- Sharma et al. [84] proposed a highly integrated amine-based CO_2 capture power plant in which a solar thermal plant provides heat in order to avoid steam extraction from HP and IP turbines, which increases power production. By means of a Heat Exchanger Network (HEN) analysis, where the compressed gas energy is also utilized in the integration process, a significant reduction of power plant output penalty is achieved (efficiency is increased up to 34.9 % from 29.4% for the base case).

Comentado [U3]: Efficiency, penalty??

In the case of CaL process, recent works have assessed the use of CSP to support CaL-based PCC for retrofitting fossil fuel power plants:

- Zhang et al. [85] evaluated the energy efficiency of the CaL system when the calciner is driven by a combination of oxy-fuel combustion and CSP, which provides 101 MW_{th} (a 7.4% of the total energy input in the calciner). An integration of the CCR process into an ultra-supercritical 1019 MW_{th} power plant was proposed. In this scheme, a fraction of the CO_2 leaving the calciner was used as a heat transfer fluid in the solar collectors after which it is recycled to the calciner. Fossil fuel consumption in the calciner was reduced by 6.9 g/kWh compared to the coal-driven case, which entails a decrease of the additional CO_2 generated and a decrease of the mass flow rate of fresh limestone makeup. This scheme leads to an overall efficiency penalty of 9.63% points associated to the CO_2 capture process. The thermal efficiency of co-driven case is just 0.28% points below that of the conventional coal-driven case (without CSP) due to the big losses of solar radiation to thermal conversion, which hinders the CSP efficiency. Accordingly, increasing the CSP capacity reduces coal consumption, but it greatly decreases the thermal efficiency due to the decrease of CSP efficiency.
- Zhai et al. [86] analyzed the CaL-PCC integration partially assisted by CSP for retrofitting existing CFPPs in order to recover the energy of the capture system. The work analyzes the integration through two different strategies, i) CFPP with solar aided CO_2 capture system ((solar + CC) + PP), which uses solar energy to reduce the fuel consumption in the calciner (a similar case than in [85]), and ii) solar aided CFPP plant with CO_2 capture system ((solar + PP) + CC) where solar energy is used in the main cycle for increasing power production. In both cases the solar thermal power available for the cycle is 88.58 MW_{th}. Results show that the second case is more beneficial regarding technical and environmental aspects, whereas the first case ((solar + CC) + PP) achieve a thermal efficiency slightly higher than in the ((solar + PP) + CC) case (31.20% against 31.09%).
- Tregambi et al. [87] assessed the performance of coupling the CaL system to CSP for a 100MW_{th} CFPP with the aim of providing all the thermal energy required in the calciner by renewable energy. The maximum thermal energy needed in the calciner to be provided entirely by CSP was 135 MW_{th}. As a novelty, the plant allows storing the excess power produced during the daytime as CaO resulting from the endothermic $CaCO_3$ calcination reaction, which could be recovered from the exothermic CaO carbonation reaction during the nighttime. They concluded that the CO_2 capture efficiency reaches a value close to 90% whereas 80% of the thermal input from the CSP system to the calciner can be recovered.

4. Detailed analysis on Dry-Carbonate Process

In the rest of this work the use of an abundant and cheap material such as sodium carbonate (Na_2CO_3) with a high dry CO_2 sorption capacity at relatively low temperatures is analysed.

~~5.1~~4.1 Description

CO_2 is captured in the Dry Carbonate Process through the chemical binding of CO_2 to Na_2CO_3 in the carbonator reactor at operating temperatures below 100°C. Na_2CO_3 is converted to $NaHCO_3$ through

the chemical reaction with CO_2 in the presence of steam. The sorbent is regenerated back to its carbonate form when heated at temperatures above 100ºC, thus releasing a nearly pure CO_2 stream after steam condensation. The design of the Dry Carbonate Process takes into account the need to periodically replenish a certain amount of sorbent makeup due to particle attrition and the loss of sorbent activity by the irreversible reaction with SO_2 and HCl. It should be noted however that in post- wet flue gas desulfurization, SO_2 and HCl are present in the flue gas at very low concentrations (less than 20 ppm for SO_2 and 1 ppm for HCl), which would require a lower amount of fresh sorbent makeup flow. Figure 2 shows a schematic flow diagram of the Dry Carbonate process.

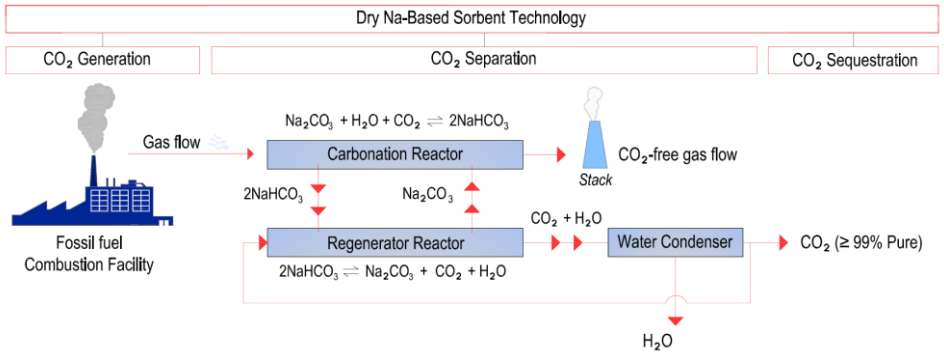

Figure 2: General scheme of the Dry Carbonate Process.

The Dry Carbonate Process is particularly well suited for being retrofitted into CFPPs with wet flue gas desulfurization and for natural gas–fired power plants. In the work conducted by Nelson et al. [74] it was estimated that a commercial-scale Dry Carbonate Process (a 500 MW_e nominal power plant fed with natural gas and carbon) would require an initial sorbent loading of roughly 387 tons and a makeup rate of fresh sorbent of about 0.2 tons/h. After integration of the Dry Carbonate Process, the net efficiency of the plant would suffer a drop from 40.5% to 33.4% (7.1 % penalty). In the case of power plants fed only with coal, there is a larger concentration of CO_2 in the flue gas and a larger amount of sorbent for CO_2 capture is needed whereas a similar loss of efficiency is expected.

The reactions involved in the capture of CO_2 using Na_2CO_3 result in the reversible formation of $NaHCO_3$ and Wegscheider's salt ($Na_2CO_3 \cdot 3NaHCO_3$) according to Eqs. 3-4 [74]:

$$Na_2CO_{3(s)} + CO_{2(g)} + H_2O_{(g)} \leftrightarrows 2NaHCO_3 \qquad \Delta H = -135.56 \frac{kJ}{mol} \qquad (3)$$

$$Na_2CO_{3(s)} + 0{,}6\ CO_{2(g)} + 0{,}6\ H_2O_{(g)} \leftrightarrows 0{,}4\ \left[Na_2CO_3 3NaHCO_{3(s)} \right] \quad \Delta H = -135.98 \frac{kJ}{mol} \qquad (4)$$

Other possible reaction byproducts, such as sodium sesquicarbonate ($Na_2CO_3 \cdot NaHCO_3 \cdot 2H_2O$) and sodium bicarbonate hydrate ($NaHCO_3 \cdot 2H_2O$) are negligible at the reaction conditions of interest. Both forward reactions are exothermic. Therefore, heat integration is important for an efficient

implementation of the process in a commercial system. Thermodynamically, the formation of Wegscheider's salt is favored under practical H_2O and CO_2 partial pressures at reaction temperatures of 70°C and above. For regeneration of the sorbent, $NaHCO_3$ decomposes to Na_2CO_3, H_2O and CO_2 in the temperature range of 100 °C–200 °C [88] although ideally fast conversion is reached at 200°C [89].

Multicycle carbonation/regeneration tests reported in [74] show the results plotted in Figure 3 for Na_2CO_3 conversion as a function of the cycle number (carbonation at 60ºC and regeneration at 160ºC). Even though further thermogravimetric analysis tests should be carried out including a larger number of cycles and analyzing also the reaction kinetics, these results suggest that conversion is kept stable at a relatively high level (around 0.9), which may be explained by the relatively low temperatures used for sorbent regeneration.

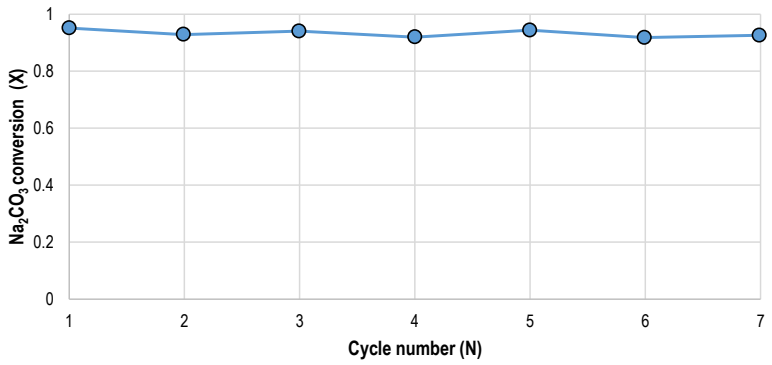

Figure 3: Na_2CO_3 conversion as a function of the cycle number (data extracted from [74]).

Potential contaminants present in the flue gas, such as SO_2 and HCl, could react irreversibly with Na_2CO_3 at process conditions according to the following reactions (Eq. 5-6):

$$Na_2CO_3 + 2HCl \leftrightarrows 2NaCl + CO_2 + H_2O \qquad (5)$$

$$Na_2CO_{3_{(s)}} + SO_{2_{(g)}} + \frac{1}{2}O_{2_{(g)}} \leftrightarrows Na_2SO_4 + CO_2 \qquad (6)$$

Formation of NaCl and Na_2SO_4 reduces the capacity of the sorbent for CO_2 capture in subsequent cycles. However, the relative concentrations of HCl and SO_2 are one order of magnitude lower than the CO_2 concentration present in the flue gas following wet FGD (flue gas desulfurization) treatment, which mitigates the irreversible loss of conversion due to this issue.

5.24.2 Chemistry of the process

In order to gain further understanding of the dry carbonation process, the reaction mechanisms of Na_2CO_3 carbonation are detailed in this section. A possible mechanism by which Na_2CO_3 reacts with CO_2 is (Eq. 7-10) [9]:

$$CO_2 + 2H_2O \rightarrow H_3O^+ + HCO_3^- \quad (7)$$

$$HCO_3^- + H_2O \rightarrow H_3O^+ + CO_3^- \quad (8)$$

$$Na_2CO_3 \rightarrow 2Na^+ + CO_3^- \quad (9)$$

$$Na^+ + HCO_3^- \rightarrow NaHCO_3 \quad (10)$$

If the gas contains SO_2 other reactions would occur in the carbonation process. SO_2 can dissolve into water yielding sulfurous acid (H_2SO_3), and then the sulfurous acid dissociates, forming H^+ and HSO_3^- (Eq. 11):

$$SO_{2(g)} + H_2O \rightarrow H_2SO_3 \rightarrow H^+ + HSO_3^- \quad (11)$$

Meanwhile, before the gas is dissolved into water, part of the SO_2 can react with O_2 to form SO_3, after which the SO_3 gas may dissolve into water to form sulfuric acid, which dissociates to H^+ and SO_4^{2-} ions leading to a reduction of the solution pH value. In addition, sulfurous acid (H_2SO_3) can also react with O_2 to form sulfuric acid. These reactions are given by Eqs. 12-14:

$$2SO_{2(g)} + O_{2(g)} \rightarrow 2SO_{3(g)} \quad (12)$$

$$SO_{3(g)} + H_2O \rightarrow H_2SO_{4(aq)} \rightarrow 2H^+ + SO_4^{2-} \quad (13)$$

$$2H_2SO_{3(aq)} + O_{2(g)} \rightarrow 2H_2SO_{4(aq)} \rightarrow 4H^+ + 2SO_4^{2-} \quad (14)$$

Also, chlorine present in the flue gas could react with water to form H_3O^+ and Cl^- (Eq. 15):

$$HCl + H_2O \rightarrow H_3O^+ + Cl^- \quad (15)$$

Besides, part of Na^+ could react with SO_4^- and Cl^- according to Eq. 16-17:

$$Na^+ + SO_4^- \rightarrow NaSO_4 \quad (16)$$

$$Na^+ + Cl^- \rightarrow NaCl \quad (17)$$

In order to model accurately the process, equilibrium reactions and salts formation were implemented in the computational model of our work. The salts formation reactions that can occur are (Eq. 18-21):

$$2Na^+ + CO_3^- + 10\,H_2O \rightarrow Na_2CO_3 \cdot 10H_2O \quad (18)$$

$$2Na^+ + CO_3^- + 7H_2O \rightarrow Na_2CO_3 \cdot 7H_2O \quad (19)$$

$$2Na^+ + CO_3^- + H_2O \rightarrow Na_2CO_3 \cdot H_2O \quad (20)$$

$$3Na^+ + CO_3^{--} + HCO_3^- + 2H_2O \rightarrow 2(Na_2CO_3 \cdot NaHCO_3 \cdot 2H_2O) \quad (21)$$

Thus, in addiction to sodium bicarbonate ($NaHCO_3$) other salts can be formed from the reactions involving CO_2, water and soda ash: sodium carbonate decahydrate ($Na_2CO_3{\cdot}10H_2O$), sodium carbonate heptahydrate ($Na_2CO_3{\cdot}8H_2O$), sodium carbonate monohydrate ($Na_2CO_3{\cdot}H_2O$), Wegscheider's salt ($Na_2CO_3{\cdot}3NaHCO_3$) and trona ($Na_2CO_3{\cdot}NaHCO_3{\cdot}2H_2O$) [90]. Figure 4 shows the evolution of reaction equilibrium constants with temperature for the production of $NaHCO_3$ and other salts used in this work (adapted from [9]). The data was well fitted to the equation

Comentado [U4]: Poner eq.

Best fitting parameters are shown in [90].

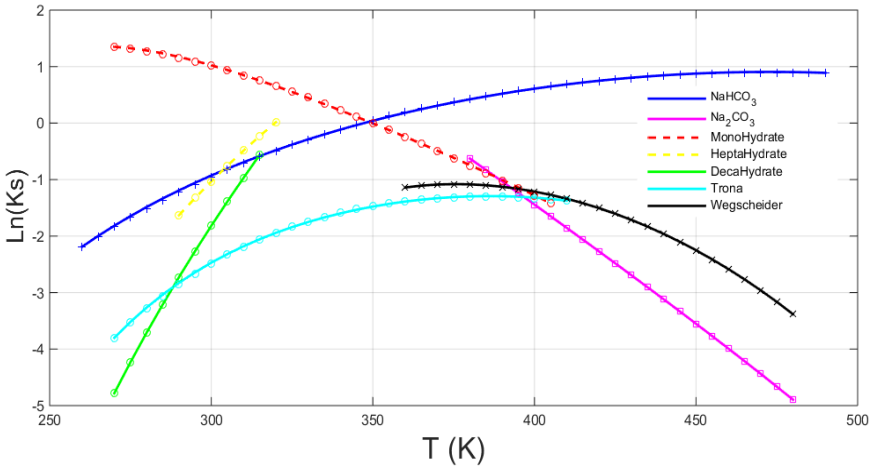

Figure 4: Ln(Ks) values for reactions involved in $NaHCO_3$ production (see for additional details)

Comentado [U5]: Citar 90

~~6.~~5. Case study: CFPP- Dry-carbonate process (DCP) integration

~~6.1~~5.1 Baseline CFPP

This section shows results from the simulation of the retrofitting of a 150 MW_e CFPP with a Dry Carbonate CO_2 capture system to assess the effects on the power plant and global system performance and to assess the feasibility of assisting sorbent regeneration by solar thermal energy.

Flue gas exiting the power plant is characterized by a dilute concentration of CO_2 and a large volumetric flow at ambient pressure. Thus, a typical 505 MW_e pulverized CFPP plant produces 28300 m^3 of flue gas per minute with a CO_2 volume concentration between 10% and 15% [91]. In this work, a reference coal fired plant of 150 MW_e has been considered. The reference plant scheme is illustrated in Figure 5 taking as a reference the integration model developed by Ortiz et al. [92]. The main data of the CFPP are given in Table 1.

Table 1: Reference data for a 150 MW_e coal fired plant (data scaled from [48]).

Item	Magnitude	Unit
Coal consumption	61	ton/hr
Air intake	692	ton/hr
Gross power introduced with fuel	447	MW_{th}
Net power supplied	397	MW_{th}
Net Power produced	150	MW_e
Net efficiency	33.5	%

Post-combustion flue gas characteristics are detailed in Table 2:

Table 2: Flue gas flow for a 150 MW_e coal fired plant (data scaled from [48]).

Coal flue gas component	Mole Flow (kmol/hr)	Mass Flow (tons/hr)
N_2	17154.21	529.71
CO_2	3085.62	135.96
H_2O	1471.86	29.4
O_2	781.8	27.57
CO	140.7	3.93
NO	135.36	4.47
SO_2	37.53	2.64

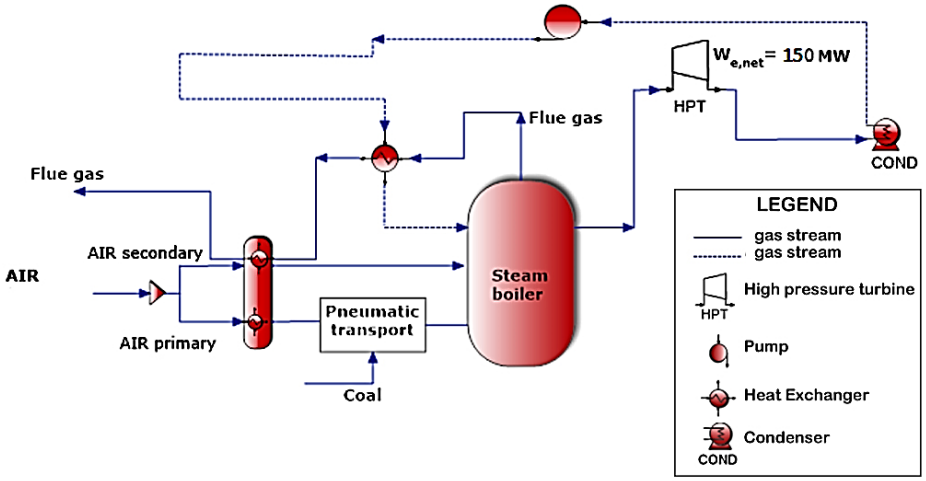

Figure 5: Reference coal fired power plant scheme used in the present work.

~~6.25.2~~ Dry Carbonate Process (DCP) integration

A schematic representation of the integrated process for CO_2 capture proposed in this work is shown in Figure 6. Simulations were done using ASPEN PLUS^{TM} environment. Main units are indicated in the layout: for carbonation (CARB) and decarbonation (DECARB) of the sorbent, two separation units and heat exchangers for heat recovery and water condensation at the end of the process are implemented. In the carbonator, inlet streams are water (WATHOT), sodium carbonate (NA_2CO_3) and cooled flue gas (FGPLAN4). The following assumptions have been considered in the simulation in ASPEN: i) ideal gas-solid separation, ii) auxiliaries are enough to heating and cooling necessities along the plant, iii) auxiliaries electric power consumption, iv) steady state operation is assumed, v) regenerator reactor model is based on chemical and phase equilibrium through Gibbs' free energy minimization method and iv) 90% isentropic efficiency is considered in the CO_2 compressor.

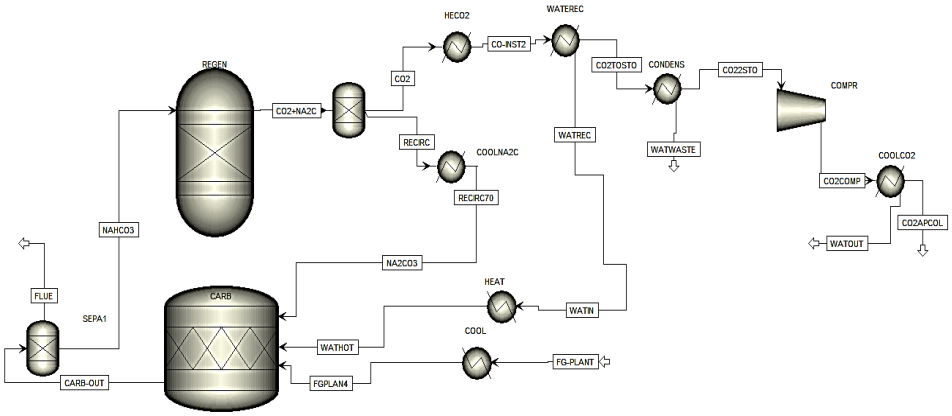

Figure 6: Dry Carbonate Process layout.

The carbonator works at 60°C and absolute pressure 1.01 bar for CO_2 sorption. Under these conditions, formation of Weigscheider' salt is thermodynamically favored. The CO_2 input flow to the carbonator (FGPLANT) is 136 ton/hr (3080 kmol/hr) while the CO_2 output flow (CARB-OUT) is 10.7 ton/hr CO_2. Efficiency of CO_2 capture in the carbonator is evaluated as:

$$\varepsilon_{ABS} = \frac{\dot{m}_{CO2,FGPLANT} - \dot{m}_{CO2,CARB-OUT}}{\dot{m}_{CO2,FGPLANT}} = 0{,}92$$

Here ε_{ABS} is the efficiency of absorption, while $m_{CO2,\ FGPLANT}$ and $m_{CO2,\ CARB.OUT}$ represent the CO_2 mass flows of flue gas exiting the CFPP and the carbonator, respectively.

Assuming a conservative value for Na_2CO_3 conversion (X=0.75) in the carbonator ([74], see Figure 3), the required mas flow of Na_2CO_3 is 430 ton/hr, which yields a mass ratio Na_2CO_3/CO_2 of 3.2 kg_{Na2CO3}/kg_{CO2}. In the best scenario (X=1), this mass ratio would be 2.4 kg_{Na2CO3}/kg_{CO2}. Na_2CO_3 carbonation proceeds at an equimolar amount of CO_2 and H_2O, which yields a hot water requirement of at least 55.4 ton/hr. Within this amount, 27 ton/h are taken directly from the residual steam in the

post-combustion flue gas while the rest must be added from an external source. Table 3 shows the values of main operation parameters in the carbonator and calciner reactors.

Table 3: Carbonator and calciner working conditions.

	carbonator	calciner
Outlet temperature [°C]	60	140
Outlet pressure [bar]	1,01	1.01
Net heat duty [MW_{th}]	-101.240	122.480
Total feed stream CO2 flow [ton/h]	135.550	0
Total product stream CO2 flow [ton/h]	10.620	127.010
Net stream CO2 production [ton/h]	-124.930	127.010

Following the proposed layout (Figure 6), the solids stream consists of $Na_2CO_3 \cdot 3NaHCO_3$ since $NaHCO_3$ and H_2O (NAHCO3C) is separated in the first separation unit from air and flue gas (FLUE) and is sent to the regenerator. Sorbent regeneration is carried out in this reactor, which releases a CO_2 concentrated stream. The amount of CO_2 released in the regenerator is 127 ton/h at 140°C with a 100% efficiency of CO_2 stripping from the sorbent.

From the energy balance in the regenerator, it may be calculated that a total 122.48 MW_{th} are required for maintaining the process. This heat can be obtained by burning additional coal or from another external source. In this work, the novel use of solar thermal power is proposed for that purpose. Pressurized hot water can be stored for a relatively long time at temperatures above 140ºC. Table 4 details the balances between the input and output flows in the calciner. It must be taken into account that part of the sorbent is lost during the overall process because of the irreversible reactions with SO_2 and HCl at the process conditions (Eqs. (5) - (6)). The loss of sorbent requires a make-up flow of 3 ton/h of Na_2CO_3 in order to maintain the capture efficiency in the carbonator. After the regeneration stage, Na_2CO_3 is separated from the gas stream and it is recirculated into the carbonator at 80ºC.

Table 4: Calciner streams composition.

	CO_2+NA	$NAHCO_3H$
Temperature (°C)	140	60
Pressure (bar)	1.01	1.01
Mass flow (ton/hr)		
H_2O	50.28	1.44
CO_2	124	0
Na_2CO_3	323.25	442.7
$NaHCO_3$	0	11.39
Wegsheider's salt		44.39

From the calciner, a gas flow of 17.8 ton/h (29% steam and 71% CO_2 by weight) is sent to a train of heat exchangers/coolers for heating and H_2O recovery. Finally, a flow of 12.7 ton/hr of pure CO_2 is compressed through three intercooled stages up to 70 bar, with a global power consumption of 1.5 MW_e, after which it is sent to storage. Considering the energy needed in the regenerator for sorbent regeneration, integration of the DCP yields a plant efficiency given by Eq. 22:

Comentado [U6]: Usamos este acrónimo en la intro, creo que mejor seguir usándolo

Comentado [U7R6]:

$$\eta_{plant} = \frac{\dot{W}_{CFPP} - \dot{W}_{cons,DC}}{\dot{Q}_{CFPP} + \dot{Q}_{DC}} \qquad (22)$$

Here η_{plant} is the plant efficiency, W_{CFPP} and Q_{CFPP} are the net power production and the thermal power consumptions of the CFPP, while $W_{cons,\,DC}$ and Q_{DC} are the electric power consumption and the thermal power consumption in the DCP, respectively. By considering the work for CO_2 compression (W_{COMP}) and solids conveying (Wsolid), parasitic power consumption ($W_{cons,DC}$) is given by Eq. 23:

$$\dot{W}_{cons,DC} = \dot{W}_{solid} + \dot{W}_{COMP} \qquad (23)$$

Here a conservative value of W_{solid} =5.5 kWh/ton can be used for estimating the solids conveying energy [93], which yields (Eq. 24):

$$\dot{W}_{solid} = \dot{m}_{Na2CO3} \cdot 5{,}5 \frac{kwh}{ton} = 2.37\ MWel \qquad (24)$$

being Na_2CO_3 the sodium carbonate mass flow. A summary of the global plant data is given in Table 5.

Table 5: Power balance without heat recovery.

	Power production	Power consumption
CFFP	150 MW_e	447 MW_{th}
Decarbonator		122.5 MW_{th}
COMP		15 MW_e
Wsolid		2.37 MW_e
Net Power	132.53 MW_e	
Total heat requirement		569.5 MW_{th}

By considering the extra-heat that must be supplied from coal to integrate the DCP, the global plant efficiency drops from 33.5% to 23.3 %. The results obtained by imposing different carbonator and regenerator temperatures are shown in Figure 7.

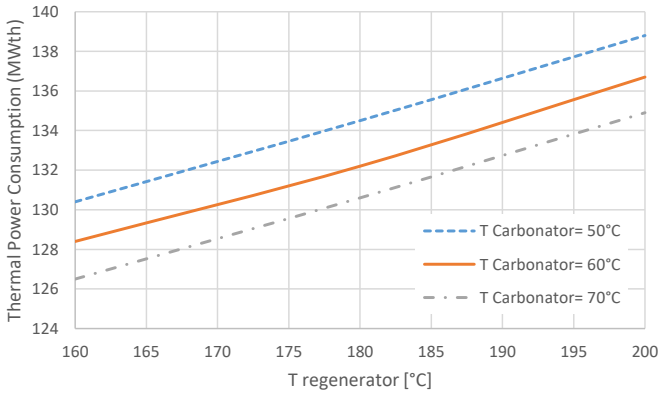

Figure 7: Thermal power required for different carbonator and regenerator temperatures.

In the temperature range 50-70 ºC for the carbonator, power consumption varies within the range 126.5MW_{th} – 138.8 MW_{th}. As will be seen below, integration of solar thermal power to aid sorbent regeneration, as newly proposed in this work, serves to mitigate significantly this significant loss of efficiency.

~~6.3~~5.3 Optimized plant configuration

The modified configuration proposed in this section is schematized in Figure 8. A solid-solid heat exchanger (HEATEXCH) has been included between the two reactors with the aim of reducing the total amount of heat required in the regenerator. This heat exchanger allows for increased temperatures in the regenerator, which enhances the reaction rate with little additional expense of thermal power. The modified configuration also leads to a reduction of the power consumption for compression by introducing a multi-stage compression with inter-refrigeration included. A sensitivity analysis using this configuration has been also carried out to analyze the variation of power required for different carbonator/regenerator temperatures (Fig. 9).

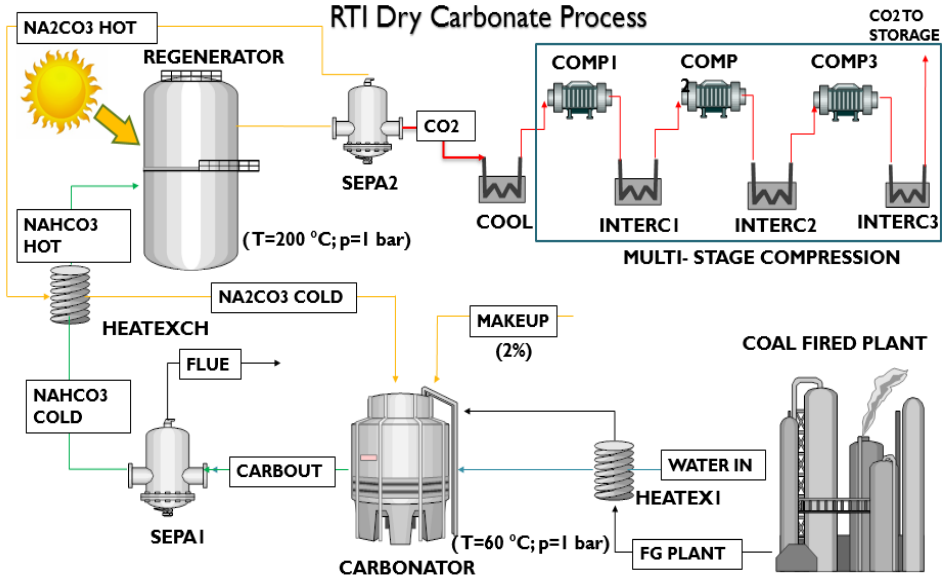

Acronyms (equipment and streams):

CARBONATOR: CO_2 capture reactor
CARBOUT: Final product from carbonator
CO_2: CO_2 recovered from the system
CO_2 TO STORAGE: CO_2 to the storage system (20 °C, 75 bar)
COAL FIRED PLANT: Coal fired plant for electricity production
COMP1: Compressor CO_2 (1-10 bar)
COMP2: Compressor CO_2 (10-25 bar)
COMP3: Compressor CO_2 (25-75 bar)
COOL: CO2 (20°C) intercooler
FGPLANT: Flue gas exits the coal fired plant
NA2CO3 COLD: Regenerated Na_2CO_3 (80°C)
NA2CO3 HOT: Regenerated Na_2CO_3 (200°C)
NAHCO3 COLD (fig.6): Solids exits the carbonator (60°C)
NAHCO3 HOT: Solids entering the regenerator (140°C)
HEATEX1 H_2O-flue gas heat exchanger
HEATEXCH: $NaHCO_3$-Na_2CO_3 heat exchanger
INTERC1: CO_2 (20°C) intercooler
INTERC2: CO_2 (20°C) intercooler
INTERC3: CO_2 (20°C) intercooler
MAKE UP: Sorbent Make up
REGENARATOR: Sorbent regenerator
SEPA1: Solid-gas separator
SEPA2: Solid-gas separator
WATER IN: Water to CO_2 capture reactor

Figure 8: Optimized plant configuration proposed in this work.

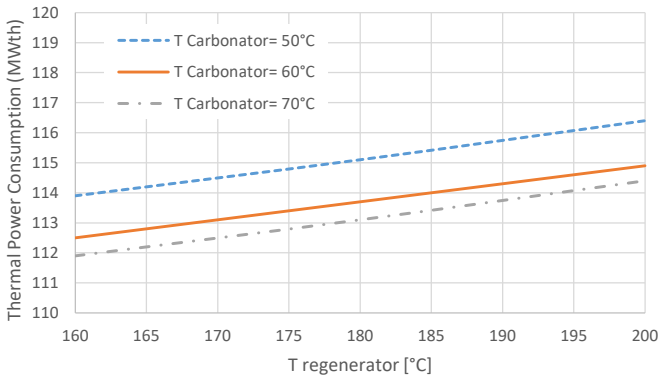

Figure 9: Power consumption for different operating conditions (including heat recovery).

In this case, the analysis shows (Figure 9) that power consumption is in the range 111.9 MW_{th} – 116.4 MW_{th}. In this new configuration, it is possible to increase temperature in the regenerator with just a slight increase of power consumption and the advantage of enhancing reaction kinetics. Thus, heat recovery reduces the heat required for sorbent regeneration by about a 10%. The heat required using this new configuration (with working conditions in the regenerator set to 200 °C and 1,01 bar) is 114 MW_{th}.

The integration of solar thermal heat for aiding sorbent regeneration is a feasible option to achieve the required temperatures in the regenerator. This renewable heat source support would mitigate significantly the operational expenditure (OPEX) penalty associated to the carbon capture system integration.

In order to minimize the power consumption of CO_2 compression a multistage compression system is proposed. Configurations with two and three stages and different compression ratios were considered, Table 6. A three-stage compression with an inter-refrigeration stage at 20°C reduces the compression power from 15 MW_e (baseline case) to 11.16 MW_e

Table 6: CO_2 compression power

	two-stage compression		three-stage compression	
Component	Exhaust Pressure (bar)	Power (MW_e)	Exhaust Pressure (bar)	Power (MW_e)
COMP1	9	6.29	4.2	3.78
COMP2	75	6.02	17.6	3.78
COMP3	-	-	75	3.6
Global W_{comp}		**12.31**		**11.16**

Table 7 shows power consumption in the different parts of the system after introducing the proposed modifications:

Table 7: Global plant energy balance.

	Power production	Power consumption
CFFP	150 MW_e	447 MW_{th}
Decarbonator		114.9 MW_{th}
COMP		11.16 MW_e
Wsolid		2.47 MW_e
Net Power	136.37 MW_e	
Total heat		561.9 MW_{th}

With these modifications, the global efficiency of the plant (coal power plant + CCS) is increased by a 0.9% (from 23.3% to 24.2%). In the above calculations, a constant value of sorbent conversion X=0.75 was used. Table 8 shows the effect of sorbent conversion (X) on global efficiency. This parameter should be determined with further certainty from lab-scale thermogravimetric studies under realistic process conditions such as the solids residence time in the reactors in future works. Nevertheless, the efficiency variation is just around 1% in a wide range of sorbent conversions (between 0.4 and 0.95, Table 8).

Table 8: Efficiency values for different sorbent conversion factors (X).

X	Na_2CO_3 flow (kmol/hr)	Calciner (MW_{th})	Carbonator (MW_{th})	W_{solid} (MW_e)	Efficiency (%)
0.4	84.5	119.5	-104	4.6	23.2
0.75	42.93	114.9	-101	2.47	24.2
0.95	32.86	111	-98	1.89	24.37

To achieve a near to zero CO_2 emissions global system, renewable energy must be used for heating the regenerator, either solar or biomass when there is no availability of solar direct irradiation, which may be accomplished by storing heat. A number of storage materials for sensible storage systems are listed in Table 9. Solid storage and liquid storage media are presented for indirect storage of thermal energy, i.e. thermal energy from a heat transfer fluid (e.g. thermal oil, air) is transferred to a solid storage medium [94] .

Table 9: Main properties of materials to store energy in the form of sensible heat [95,96]

	Temperature (°C) Cold	Hot	Average density (kg/m³)	Average heat conductivity (W/(mK))	Average heat capacity (kJ/(kgK))	Thermal diffusivity (m²/s)	Volume specific heat capacity (kWht/m³)	Volume (m³)
Solid storage media								
Sand-rock-mineral oil	200	300	1700	1.0	1.30	4.5×10-7	60	22460.1
Reinforced concrete	200	400	2200	1.5	0.85	8.0×10-7	100	13271.9
Cast iron	200	400	7200	37.0	0.56	9.2×10-6	160	6155.4
Liquid storage media								
Mineral oil	200	300	770	0.12	2.6	6.0×10-8	55	24793.6
Synthetic oil	250	350	900	0.11	2.3	5.3×10-8	57	23979.1
Silicone oil	300	400	900	0.10	2.1	5.3×10-8	52	Out of range
Nitrite salts	250	450	1825	0.57	1.5	2.1×10-7	152	Out of range

For this study, the storage volume needed for supplying the heat for regeneration during 12 hours has been estimated. For example, a volume of 25m x 25m x 10m is required for cast iron in order to cover a storage capacity of 12 hours while if sand-rock mineral oil is used the volume needed is 50m x 50m x 10m (Table 9). Storage capacity has been estimated including a utilization coefficient $f_{utilisation}$. This factor depends on the heat conductivity of the storage medium and the operational mode of the storage [95]:

$$Q_{storage} = f_{utilization} \times m \times c_p \times \Delta T_{mix/max} \quad (36)$$

where m is the mass [kg], c_p is the mean heat capacity [J/(kgK)] and $\Delta T_{mix/max}$ is the temperature difference of the working fluid. Estimated associated costs of the solar system are included in the economic sensitivity analyses. These volume sizes constrain the applicability of the integrated CCS/solar solution as depending on space availability.

Another possibility for achieving the near to zero CO_2 emissions global system would be using biomass to meet power requirements for the regenerator (114.9 MW_{th} in the Best Estimate case). By considering an average heat capacity of biomass of 10.87 MJ/kg (Table 10), a biomass flow rate input of 44.5 ton/h is necessary. If wood chips are used, the storage capacity for the biomass needed for one week of plant operation would be around 17500 m³.

Comentado [U8]: Todavía no hemos hablado de casos...

Table 10: Properties of different typologies of wood chips

Wood chips	H_i[MJ/kg]	ρ[kg/m³]	H_i[MJ/ m³]
Chestnut	10,53	580	6106,24
Beech	13,45	750	10084,95
Spruce	7,90	450	3556,98
Larch	11,60	660	7654,88
Average	10,87	610	6630,29

Under the Carbon Emissions Reduction Target (CERT), a factor of 0.0249 kg_{CO2}/kWh is assumed for wood [97]. In the case study a factor of 0.03 ton_{CO2}/MWh is considered. Thus, an additional amount of 3.5 ton/h (from 10.7 ton/h to 14.2 ton/h) must be taken into account in the analysis.

~~6.4~~5.4 CFPP- Dry-carbonate process integration: Economic Analysis

A detailed techno-economic analysis to assess the integration of medium temperature solar thermal technology to assist regeneration of the dry sorbent has been carried out. If heat for regenerator is obtained from solar thermal power the economic efficiency (defined in this case as the ratio between power production -136 MW_e- and fossil fuel consumption -447 MW_{th}- without considering solar thermal power) would be 30.5%. A number of assumptions according to different scenarios were made for the economic analysis. These different scenarios were defined in terms of:

- Electricity production, to take into account the penalty on electricity generation of the ancillary equipment consumption and parasitic loads (consumption in compressors, solids conveying and other ancillary equipment). All these factors have been considered by an electricity penalty of 10.1%.
- Variation of fuel costs, to include in the analyses the variability of fuel costs.
- Uncertainties in plant installation costs, to take into account uncertainty in the evolution of equipment costs. The maximum deviation has been taken as a $\pm$9% of the average installation price.
- DCP costs. As for any novel technology, there is uncertainty on the installation costs and its evolution. A range of $\pm$50% for CCS installation cost has been considered.
- Different fixed charge factors were in addition considered for the different scenarios.

Under these considerations, three scenarios were defined:

- Scenario **P** (Pessimistic Scenario). The pessimistic scenario implies a combination of the following factors: highest penalty in electricity generation (it has been taken as the maximum error in estimating parasitic electricity losses), highest costs and a fixed charge factor of 0.15.
- Scenario **BE** (Best Estimated Scenario). In this scenario, the values derived from the simulation above described were used to define the efficiency of the system. It considers a capital cost of 30 M€ [6] for the CCS technology and a fixed charge factor of 0.1.
- Scenario **O** (Optimistic Scenario). This optimistic scenario considers a range of minor fuel cost and minor costs of the CCS technology and plant installation. Furthermore, it considers the smallest change in electricity production and the smallest fixed charge factor of 0.075.

Table 11 summarizes the data used for calculating the costs according to the different scenarios for a total amount of 1089 kton/year avoided CO_2 emissions using the DCP.

Table 11: CO_2 emission data for different scenarios.

	REFERENCE PLANT	DRY CARBONATE (P)	DRY CARBONATE (BE)	DRY CARBONATE (O)
Power (MW_e)	150	150	150	150
CCS Power consumption (MW_e)	-	25	13.63	13
Regenerator Heat requirement (MW_{th})	-	119	114.9	111
Net power (MW_e)	150	125	136.37	137
CO_2 Emissions (ton/hr)	136	10.7	10.7	10.7
CO_2 Emissions (kmol/hr)	3080	243.2	243.2	243.2
CO_2 Avoided Emissions (kton/year)		1089	1089	1089
CO_2 Emissions (tons/ MWh_e/hr)	0.9	0.085	0.078	0.078

Along with capital investment and operating and maintenance (O&M) cost, energy consumption is a main factor that determines the viability of a CO_2 capture technology. The specific energy consumption for CO_2 avoided (SPECCA) is usually employed to quantify the additional fuel consumption (in MJ) needed to avoid the emission of 1 kg of CO_2 into the atmosphere [42] (Eq. 25):

$$SPECCA = 3600 \frac{\frac{1}{\eta_{CCS}} - \frac{1}{\eta_{ref}}}{E_{ref} - E_{CCS}} \quad \left[\frac{MJ}{kg_{CO2}}\right] \qquad (25)$$

where η_{ref} and η_{CCS} are the power plant efficiencies, and E_{ref} and E_{CCS} are the CO_2 emissions ratios (in kg_{CO2} /MWh_{el}) without and with the DCP integrated, respectively. Table 12 shows the results obtained from the SPECCA analysis for the different scenarios:

Table 12: SPECCA Analysis for different scenarios.

Item	Scen.P	Scen. BE	Scen. O
Net Power Production (MW_e)	125	136,37	137
$CO_{2\ CCS}$ (ton/hr)	10,7	10,7	10,7
E_{CCS} (kg_{CO2}/kWh_{el})	85.60	78.46	78.10
η_{CCS}	0.232	0.242	0.244
SPECCA (MJ/kg_{CO2})	5.86	5.03	4.90
η_{CCS_ECO}	0.279	0.305	0.306
$SPECCA_{\_ECO}$(MJ/kg_{CO2})	2.65	1.29	1.24

If the analysis is performed in terms of operational expenditures, and heat for regeneration of the sorbent is provided by solar (evaluated as a free energy intake from the point of view of OPEX), an operational efficiency value can be defined as η_{CCS_ECO}= Net Power Production with CCS (MW_e)/ fossil fuel consumption (MW_{th}). For operational expenditures analysis, a new SPECCA definition is used ($SPECCA_{ECO}$) in order to remark the difference between concepts (see Table 12):

Comentado [U9]: No se entiende...cual es la def de este nuevo specca?

The economic cost of CO_2 capture can be estimated in different ways, yet the most commonly used method contemplates incremental cost of electricity (€/kWh) and avoiding CO_2 cost (AC) expressed in terms of €/tonCO_2 avoided [98] (Eq. 26-27):

$$\Delta COE = COE_{CCS} - COE_{ref} \quad (26)$$

$$AC = \frac{\Delta COE}{\left(\frac{ton_{CO2}}{kWh}\right)_{CCS} - \left(\frac{ton_{CO2}}{kWh}\right)_{CCS}} \quad (27)$$

Here COE is the cost of electricity, the sub-index *CCS* represents the carbon capture and storage system and the sub-index *ref* refers to the reference plant (coal fired plant). For an accurate economic analysis, the lack of imposed taxes to CO_2 emissions has been taken into consideration. The costs of electricity in the three different scenarios for the reference plant are given by Eq. 28:

$$COE = fixed\ cost + variable\ cost + fuel\ cost = \frac{TCR \cdot FCF}{8760\ h} + VOM + \frac{FC}{\eta_{el}} \quad (28)$$

where η is the global plant efficiency (η = 0.335 for the reference plant).

Regarding the solar thermal power technology that would be used for producing the thermal power required for sorbent regeneration, a cost range between 1500-3500 €/kW [11] has been estimated for a parabolic trough plant with thermal energy storage [94]. This solar thermal technology can supply heat for regeneration of the dry sorbent at the required temperatures in the regenerator. Thus, to supply the heat required for the CCS system the expected cost has been calculated as (Eq. 29):

$$E_{SOLAR}(M€) = c_{SOLAR}\left(\frac{M€}{MW}\right) \cdot \Phi_{REGENERATOR}(MW) \quad (29)$$

where c_{SOLAR} is the solar plant cost and $\Phi_{REGENERATOR}$ is the thermal power required by the regenerator.

The summarized COE costs for the three scenarios are shown in Table 13:

Table 13: COE for different scenarios.

Item	Item	Units	Scen. P	Scen. BE	Scen. O
Fuel Cost [99]	FC	€/kWh	0.03	0.023	0.02
Capital Cost	TCR	€/kWe	1200	1100	1000
Fixed Charge Factor [99]	FCF	$year^{-1}$	0.15	0.1	0.075
Variable Cost	VOM	€/kWe	0.006	0.006	0.006
COE_{ref}		€/kWh	0.116	0.087	0.074

Table 14 shows the COE and investment costs for the three scenarios considered to facilitate the analysis on the effect of solar thermal power cost (in the range between 1500 €/kW_{th} and 3500 €/kWth). These include the cost of the heat storage system. Regarding the cost of electricity with a

CCS system, electric efficiency depends on power consumption for the different scenarios. Table 15 shows the variation of COE for the different solar thermal power costs.

Table 14: COE for CCS system (as function of Solar Capital Costs).

Item	Item	Units	Scen. PE	Scen. BE	Scen. O
Net Power Production		MW_e	125	136.37	137
η_{el}			27.9	29.9	30.2
η_{system}		%	22.1	24.2	24.37
Dry Carb. Capital cost [6]	TCR	M€/ MW_e	0.32	0.223	0.148
Solar Capital Cost [100]	TCR	M€/MW_e	1.5		
COECCS		€/kWh	0.165	0.115	0.095
AC		€/ton_{CO2}	60.416	34.245	25.421
Solar Capital Cost [100]	TCR	M€/ MW_e	2		
COECCS		€/kWh	0.174	0.121	0.099
AC		€/ton_{CO2}	64.223	41.188	30.629
Solar Capital Cost [100]	TCR	M€/ MW_e	2.5		
COECCS		€/kWh	0.182	0.127	0.103
AC		€/ton_{CO2}	73.736	48.132	35.837
Solar Capital Cost [100]	TCR	M€/ MW_e	3		
COECCS		€/kWh	0.191	0.132	0.108
AC		€/ton_{CO2}	83.249	55.076	41.045
Solar Capital Cost [100]	TCR	M€/ MW_e	3.5		
COECCS		€/kWh	0.199	0.138	0.112
AC		€/ton_{CO2}	92.762	62.020	46.253

Table 15: ΔCOE (€/kWh_{el}) for different costs of solar thermal field.

Solar Thermal cost (€/kW_t)	Scen. P	Scen. BE	Scen. O
1500	0.0492	0.0281	0.0209
2000	0.0578	0.0339	0.0252
2500	0.0664	0.0396	0.0295
3000	0.0749	0.0453	0.0337
3500	0.0835	0.0510	0.0380

The costs of the other components and reactors are estimated in the range between 20 and 40 M€ [6]. Finally, maintenance and operation costs are assumed as 10% of the total investment cost. The investment cost of the CCS system is given by Eq. 30:

$$E_{TOT} = E_{SOLAR} + E_{DRYCARBONATE} + E_{O\&M} \qquad (30)$$

where E_{TOT} is the total investment cost, E_{SOLAR} is the solar plant installation cost, $E_{DRYCARBONATE}$ is the carbon capture system installation cost and $E_{O\&M}$ represents the cost due to operation and maintenance. Total CFPP retrofitting investment cost are shown in Table 16 as a function of investment costs for the three scenarios and solar field prices considered.

Table 16: Total CFPP retrofitting investment cost calculated by considering several CSP plant prices.

Solar Thermal Cost 1.5 M€/ MW_e				
	Units	Scen. P	Scen. BE	Scen. O
ESOLAR	M€	179.25	172.35	166.5
EDRY	M€	40	30	20
EO&M	M€	21.92	20.23	18.65
ETOT	M€	241.17	222.58	205.15
Solar Thermal Cost 2 M€/ MW_e				
	Units	Scen. P	Scen. BE	Scen. O
ESOLAR	M€	239	229.8	222
EDRY	M€	40	30	20
EO&M	M€	27.9	25.98	24.2
ETOT	M€	306.9	285.78	266.2
Solar Thermal Cost 2.5 M€/ MW_e				
	Units	Scen. P	Scen. BE	Scen. O
ESOLAR	M€	298.75	287.25	277.5
EDRY	M€	40	30	20
EO&M	M€	33.87	31.725	29.75
ETOT	M€	372.62	348.975	327.25
Solar Thermal Cost 3 M€/ MW_e				
	Units	Scen. P	Scen. BE	Scen. O
ESOLAR	M€	358.5	344.7	333
EDRY	M€	40	30	20
EO&M	M€	39.85	37.47	35.3
ETOT	M€	438.35	412.17	388.3
Solar Thermal Cost 3.5 M€/ MW_e				
	Units	Scen. P	Scen. BE	Scen. O
ESOLAR	M€	418.25	402.15	388.5
EDRY	M€	40	30	20
EO&M	M€	45.82	43.21	40.85
ETOT	M€	504.07	475.36	449.35

After the economic evaluation of electricity costs and avoided CO_2 emissions with the DCP assisted by medium temperature solar thermal power, net present value (NPV) and Simple Pay Back (SPB) are analyzed with the goal of assessing the effects of carbon taxes and installation funds for renewables technologies. To carry out these analyses, carbon taxes are assumed as fixed through the next years in the worst scenario (Scenario P) while they are assumed to increase in future years for the optimistic scenario (Scenario O). Additionally, European or National funds could be received by the integration of solar thermal power to reduce CO_2 emissions. The net gain from avoided CO_2 emissions is given by Eq. 31:

$$E_{CO2,AVOIDED} = \left(ton_{CO2,ref} - ton_{CO2,CCS}\right) \cdot c_{CO2} \qquad (31)$$

where $E_{CO2\ AVOIDED}$ is the avoided cost due to the avoided emission of CO_2, $ton_{CO2,\ ref}$ and $ton_{CO2,\ CCS}$ are the CO_2 emissions without and with the DCP integrated, respectively, while c_{CO2} is the carbon tax expressed in €/ton_{CO2}. The energy simple payback period, SPB, is the time to recover the initial investment in energy savings. SPB is calculated as the ratio of capital costs to the annual energy cost savings (Eq. 32):

$$SPB = \frac{E_{TOT}}{E_{NET,\mathrm{GAIN},year}} \qquad (32)$$

where E_{TOT} is the total investment of the plant while $E_{NET,\ GAIN,\ year}$ represents the annual economic gain due to the avoided emissions. Figure 10 illustrates the SPB curves for the three scenarios as function of total CFPP retrofitting capital cost.

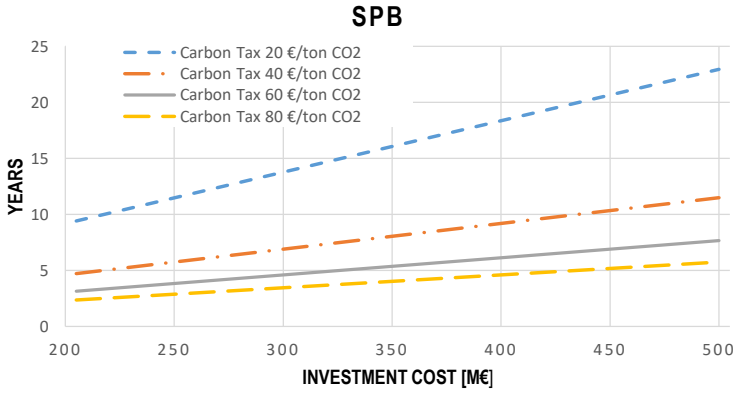

Figure 10: SPB curves according to the three scenarios as function of CFPP retrofitting capital costs.

The net present value (NPV) is calculated as the discounted cash flow minus the capital cost (Eq. 33):

$$NPV = \sum_{n=0}^{n} \frac{E_{NET,GAIN,year}}{(i+1)^n} - E_{TOT} \qquad (33)$$

where *n* represents the year number and *i* represents the discount rate. Figure 11 illustrates the variation of NPV as a function of the carbon taxes value for fixed discount rate (*i*=0.1) and different values of investment cost.

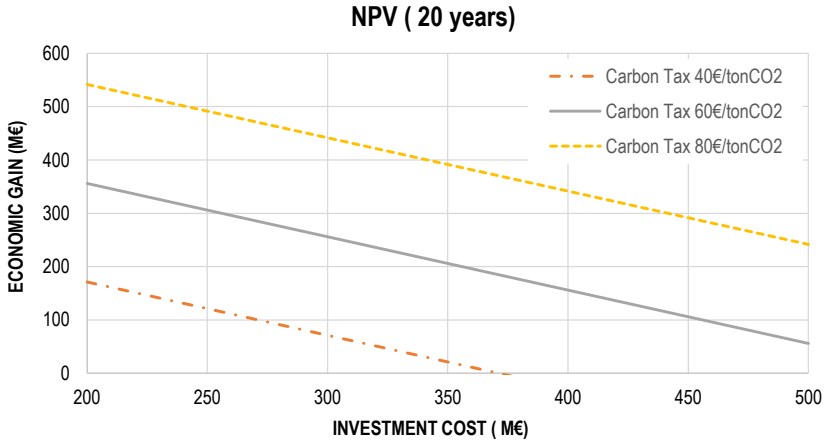

Figure 11: NPV for different carbon tax values and different investment costs.

As can be seen, NPV changes substantially under different situations of carbon taxes. In addition for solar installations there are available funds that could be considered (European or National funds) that would favor retrofitting of the plant but they have not been included in this analysis.

If the economic profit for the avoided CO_2 emissions is not enough to balance the additional investment cost an increase of electricity price ($\Delta PRICE_{EL}$) is required. The annual revenues due to this incremental cost is given by Eq. 34:

$$E_{INCR} = \Delta PRICE_{EL}\left(\frac{€}{kwh}\right) \cdot P_{NET,year}\left(\frac{MWh}{year}\right) \qquad (34)$$

where E_{INCR}, expressed in M€/year, represents the revenues due to the incremented cost of selling electricity while $P_{NET,\,year}$ is the total electric energy per year produced by the plant. Thus, the total yearly revenue ($E_{TOT,\,REV}$) would be (Eq. 35):

$$E_{TOT,REV} = E_{NET,GAIN,year} + E_{INCR} \qquad (35)$$

The required rise of electricity price associated to each case is shown in Table 17:

Table 17: Required increment of electricity sale price for maintaining a fixed value of IRR=0.1

	Total Investment Cost (M€)	E_{incr} (M€/year)	Δ Electricity price (c€/kWh)
Without Carbon Tax	200	23.5	1.967
	300	35.2	2.947
	400	47	3.934
	500	58.8	4.922
Carbon Tax 20 €/tonCO2	200	0	0
	300	11.6	0.971
	400	23.4	1.959
	500	35.2	2.947
Carbon Tax 40€/tonCO2	200	0	0
	300	0	0
	400	0	0
	500	11.5	0.963

~~6.5~~5.5 Heat storage for near zero CO_2 emissions

The use of heat storage for solar has been considered in the previous analyses by taking into account solar equipment costs. If biomass is alternatively employed, operating costs derive from the various stages of the supply chain (cutting, chipping, transportation). On average, a total cost of 50 €/ton [101] for M40 (M40= 40% of humidity) wood chip can be estimated whereas the total cost would be 85 €/ton [102] for M20 wood chip. In the case study the LHV is near a M40 wood chip class. If a wood chip price of 60 €/ton is assumed, it would result a biomass annual cost of 31.18 M€. Under a scenario of 60 €/ton CO_2 for carbon taxes a yearly revenue of 32.31 M€ could be achieved. For these calculations, a total investment cost within the range of 80-110 €/kW [103] is considered for the biomass system, where O&M costs are estimated as a 40% of the capital costs.

~~6.6~~5.6 Discussion

The above results suggest a potential interest of the DCP for CO_2 capture. The energy penalty that results from retrofitting a CFPP with this CCS technology (~9%) is similar to that estimated for other technologies such as pre-combustion CO_2 capture (~16%), amines scrubbing (~8-12%), membranes (~5-8.5%) and Calcium Looping (~4-9%). However, because of the low temperature needed to regenerate the sorbent, a CO_2 neutral solar facility could be efficiently integrated to supply the heat required, which would reduce coal consumption and operation costs significantly. Solar energy integration would serve to decrease the energy penalty just to CO_2 compression and ancillaries consumption, which leads to a near to zero CO_2 emissions power plant. The solar-CCS system penalty is estimated as just 3-4% points, with a SPECCA of only around 2 MJ/kg, which is well below the SPECCA values reported for other CO_2 capture technologies. Previous works based on thermodynamic analysis of the DCP report an energy consumption of about 3 MJ/kg [8], which is in the range of the results obtained in this work.

Comentado [U10]: Cuidado con esto...

Comentado [U11]: Cuidado con esto...

Comentado [U12]: No entiendo...arriba queremos decir que el solar ayuda a reducir significativamente el specca...y a hora decimos que en trabajos previos sin solar el specca es similar?

The results obtained from the economic analysis strongly suggest the economic viability of using the DCP to retrofit a CFPP. Since the DCP is an emerging CCS technology, cost estimations are based on assumptions based on diverse scenarios. Thus, for a 150 MW_e CFPP, the most optimistic scenario leads the total investment cost of 205 M€ whereas for the pessimistic scenario the calculated investment is 449 M€. If medium temperature solar energy is used to assist the DCP, the estimated costs are in the range between 25 and 46 €/ton_{CO2} (avoided CO_2) and from 0.095 to 0.112 € per kWh_e. According to Zhao et al. [8], the total capital cost of an Integrated Gasification Combined Cycle (IGCC) plant with a pre-combustion CO_2 capture system is about 1775-2567$/kW, the cost of a CFPP with a MEA system for post-combustion CO_2 capture would be about 1798$/kW, that of an oxy-combustion plant would be about 1810 $/kW whereas that of a membrane/catalytic plant would be 2082 $/kW. Considering the results obtained for the optimistic case, the total investment cost of the proposed solar assisted DCP is estimated in the range of 1500-3300 $/kW as function of solar facility cost. For that, the Dry Carbonate Process investment cost of 160-320€/kW, which is in the line of previous works [6,8].

It is important to point out that the above analysis is based on different assumptions for a novel integration scheme. However, the preliminary results obtained show an interesting potential to be further explored by a deeper analysis in future works. Future works should address in further depth a comparison between different CFPP-DCP-solar integration schemes to minimize energy penalty and investment costs. Since the carbonation reaction is exothermic, a proper use of the released energy is fundamental. Moreover, further work on the multicycle sorbent behavior at realistic process conditions is needed.

~~7.~~6. Conclusions

This paper is devoted in its first part to provide an overview of the currently most studied CO_2 capture systems. The performance of CCS technologies is assessed, highlighting advantages, drawbacks and challenges. In a second part a novel analysis is carried out for the integration of medium temperature solar thermal energy into the Dry Carbonate Process to assist sorbent regeneration. The Dry Carbonate Process to capture CO_2 is based on the use of a cheap, abundant and non-toxic material (Na_2CO_3) as dry sorbent at relatively low temperatures for both carbonation and sorbent regeneration. Our work shows that, when coupled with a medium temperature solar thermal power technology including thermal storage, the integration yields a nearly zero CO_2 emissions with a reduced global penalty in the power plant and avoiding also the generation of hazardous waste. The efficiency of the power plant coupled to the Dry Carbonate Process to capture CO_2 is decreased from 33.5% to 24.2% if fossil fuel is used to supply the heat for regeneration of the sorbent. This penalty is due to the amount of heat required for sorbent regeneration plus the power spent for CO_2 compression and solid conveying. If solar thermal power is used for sorbent regeneration, the penalty drops remarkably and the global efficiency, defined in terms of operational expenditures, is just decreased from 33.5% to 30%. Since additional fossil fuel would not be needed for sorbent regeneration most of this penalty is due to compression of the captured CO_2. A cost estimation of CO_2 capture by means of the Dry Carbonation Process coupled to solar thermal power (for the optimistic scenario) ranges from 25 to 46 €/ton_{CO2} (avoided CO_2) and from 0.095 to 0.112 € per kWh_e produced (compared to 0.087 €/kWh_e

Comentado [U13]: Dependerá del tamaño de planta, no?

Comentado [U14]: Arriba, sin solar, hay que poner las mismas unidades

Comentado [U15]: Arriba, sin solar, no se dicen estos costes. Habria que ponerlos para resaltar la mejora con solar

Comentado [U16]: Que son estos costes?...cuales son sin solar?

Comentado [U17]: No se entiende la comparación...son estos Kwe?...parece que estamos comparando con los valores de arriba de ~0.1 €/kWe...cuales son los costes de estas tecnología por €/tonCO2

Comentado [u18]: Revisar los valores que hay y dejar claro que es cada cosa

Comentado [U19]: La comparación es muy confusa...hay que dejarla más clara, quizás hacer una tabla y decir claramente que es cada coste

for the reference plant) as depending on the cost of the solar thermal technology. Thus, the highest costs are associated to the solar energy system. Although there is room for technology improvement and additional cost reductions could be expectedly achieved, the proposed integration based on solar thermal power and the Dry Carbonation Process can be considered as a promising technology as compared to other carbon capture technologies and renewable energy integrations recently proposed in the literature.

Acknowledgements

This work was supported by the Spanish Government Agency Ministerio de Economia y Competitividad and FEDER Funds (contracts CTQ2014-52763-C2-2-R and MAT2013-41233-R). The authors would like to thank the Spanish Ministry of Education, Culture and Sport for financial support via two pre-doctoral contracts: the FPU contract granted to Francisco Jesús Lizana Moral (FPU14/06583); and the FPI contract granted to Carlos Ortiz Dominguez (BES-2015-0703149).

References

[1] United Nations, United Nations. Framework Convention on Climate Change. Adoption of the Paris Agreement. vol. 21932. 2015.

[2] IRENA. REthinking Energy 2017: Accelerating the global energy transformation. IRENA 2017.

[3] Arnette AN. Renewable energy and carbon capture and sequestration for a reduced carbon energy plan: An optimization model. Renew Sustain Energy Rev 2016;70:254–65. doi:10.1016/j.rser.2016.11.218.

[4] Zhang X, Singh B, He X, Gundersen T, Deng L, Zhang S. Post-combustion carbon capture technologies: Energetic analysis and life cycle assessment. Int J Greenh Gas Control 2014;27:289–98. doi:10.1016/j.ijggc.2014.06.016.

[5] Annesini MC, Augelletti R, De Filippis P, Scarsella M, Verdone N. Sviluppo di un processo di separazione della CO 2 dal biogas mediante assorbimento con soluzioni amminiche in solvente organico (Report RdS/PAR2013/253). 2013.

[6] Nelson TO, Coleman LJI, Green DA, Gupta RP. The dry carbonate process: Carbon dioxide recovery from power plant flue gas. Energy Procedia 2009;1:1305–11. doi:10.1016/j.egypro.2009.01.171.

[7] Kondakindi RR, Aleksic S, Whittenberger W, Abraham MA. Na2CO3-based sorbents coated on metal foil: Post testing analysis. Top Catal 2013;56:1944–51. doi:10.1007/s11244-013-0131-1.

[8] Zhao C, Zhao C, Chen X, Anthony EJ, Jiang X, Duan L, et al. Capturing CO2 in flue gas from fossil fuel-fired power plants using dry regenerable alkali metal-based sorbent. Prog Energy Combust Sci 2013;39:515–34. doi:10.1016/j.pecs.2013.05.001.

[9] Bonaventura D, Chacartegui R, Valverde JM, Becerra JA, Verda V. Carbon capture and utilization for sodium bicarbonate production assisted by solar thermal power. Energy Convers Manag 2017. doi:10.1016/j.enconman.2017.03.042.

[10] Change WGI of the IP on C. IPCC,2005: Special Report on CARBON DIOXIDE CAPTURE AND STORAGE. 2005.

[11] International Energy Agency. Technology Roadmap Solar Thermal Electricity 2014:52. doi:10.1007/SpringerReference_7300.

[12] Jansen D, Gazzani M, Manzolini G, Dijk E Van, Carbo M. Pre-combustion CO2 capture. Int J Greenh Gas Control 2015;40:167–87. doi:10.1016/j.ijggc.2015.05.028.

[13] Feron PHM, Hendriks CA. CO2 Capture Process Principles and Costs. Oil Gas Sci Technol – Rev IFP 2005;60:451–9. doi:10.2516/ogst:2005027.

[14] Chacartegui R, Torres M, Sánchez D, Jiménez F, Muñoz a., Sánchez T. Analysis of main gaseous emissions of heavy duty gas turbines burning several syngas fuels. Fuel Process Technol 2011;92:213–20. doi:10.1016/j.fuproc.2010.03.014.

[15] Chacartegui R, Sánchez D, de Escalona JMM, Monje B, Sánchez T. On the effects of running existing combined cycle power plants on syngas fuel. Fuel Process Technol 2012;103:97–109. doi:10.1016/j.fuproc.2011.11.017.

[16] Sánchez D, Chacartegui R, Muñoz A, Sánchez T. Thermal and electrochemical model of internal reforming solid oxide fuel cells with tubular geometry. J Power Sources 2006;160:1074–87. doi:10.1016/j.jpowsour.2006.02.098.

[17] IEAGHG. CO2 Capture at Gas Fired Power Plant. 2012.

[18] Barelli L, Bidini G, Gallorini F, Servili S. Hydrogen production through sorption-enhanced steam methane reforming and membrane technology: A review. Energy 2008;33:554–70. doi:10.1016/j.energy.2007.10.018.

[19] Perejon A, Romeo LM, Lara Y, Lisbona P, Valverde JM. The Calcium-Looping technology for CO2 capture: On the important roles of energy integration and sorbent behavior. Appl Energy 2015;162:787–807. doi:10.1016/j.apenergy.2015.10.121.

[20] Ochoa-Fernandez E, Haugen G, Zhao T, Ronning M, Aartun I, B?rresen B, et al. Process design simulation of H2 production by sorption enhanced steam methane reforming: evaluation of potential CO2 acceptors. Green Chem 2007;9:654. doi:10.1039/b614270b.

[21] Martínez I, Romano MC, Chiesa P, Grasa G, Murillo R. Hydrogen production through sorption enhanced steam reforming of natural gas: Thermodynamic plant assessment. Int J Hydrogen Energy 2013;38:15180–99. doi:10.1016/j.ijhydene.2013.09.062.

[22] Ramkumar S, Fan LS. Calcium looping process (CLP) for enhanced noncatalytic hydrogen production with integrated carbon dioxide capture. Energy and Fuels 2010;24:4408–18. doi:10.1021/ef100346j.

[23] Wall T, Liu Y, Spero C, Elliott L, Khare S, Rathnam R, et al. An overview on oxyfuel coal combustion-State of the art research and technology development. Chem Eng Res Des 2009;87:1003–16. doi:10.1016/j.cherd.2009.02.005.

[24] Pei X, He B, Yan L, Wang C, Song W, Song J. Process simulation of oxy-fuel combustion for a 300 MW pulverized coal-fired power plant using Aspen Plus. Energy Convers Manag 2013;76:581–7. doi:10.1016/j.enconman.2013.08.007.

[25] Chen L, Yong SZ, Ghoniem AF. Oxy-fuel combustion of pulverized coal : Characterization , fundamentals , stabilization and CFD modeling. Prog Energy Combust Sci 2012;38:156–214. doi:10.1016/j.pecs.2011.09.003.

[26] Kather A, Scheffknecht G. The oxycoal process with cryogenic oxygen supply. Naturwissenschaften 2009;96:993–1010. doi:10.1007/s00114-009-0557-2.

[27] Scheffknecht G, Al-Makhadmeh L, Schnell U, Maier J. Oxy-fuel coal combustion-A review of the current state-of-the-art. Int J Greenh Gas Control 2011;5:16–35. doi:10.1016/j.ijggc.2011.05.020.

[28] Seepana S, Jayanti S. Steam-moderated oxy-fuel combustion. Energy Convers Manag 2010;51:1981–8. doi:10.1016/j.enconman.2010.02.031.

[29] Romano M, Martínez I, Murillo R, Arstad B. Guidelines for modeling and simulation of Ca-looping processes. 2012.

[30] Martínez I, Murillo R, Grasa G, Abanades JC. Integration of a Ca-looping system for CO2 capture in an existing power plant. Energy Procedia 2011;4:1699–706. doi:10.1016/j.egypro.2011.02.043.

[31] Posch S, Haider M. Optimization of CO2 compression and purification units (CO2CPU) for CCS power plants. Fuel 2012;101:254–63. doi:10.1016/j.fuel.2011.07.039.

[32] Romano MC. Ultra-high CO2 capture efficiency in CFB oxyfuel power plants by calcium looping process for CO2 recovery from purification units vent gas. Int J Greenh Gas Control 2013;18:57–67. doi:10.1016/j.ijggc.2013.07.002.

[33] Escudero AI, Espatolero S, Romeo LM. Oxy-combustion power plant integration in an oil refinery to reduce CO2 emissions. Int J Greenh Gas Control 2016;45:118–29. doi:10.1016/j.ijggc.2015.12.018.

[34] Buhre BJP, Elliott LK, Sheng CD, Gupta RP, Wall TF. Oxy-fuel combustion technology for coal-fired power generation. Prog Energy Combust Sci 2005;31:283–307. doi:10.1016/j.pecs.2005.07.001.

[35] Escudero AI, Espatolero S, Romeo LM, Lara Y, Paufique C, Lesort A-L, et al. Minimization of CO2 capture energy penalty in second generation oxy-fuel power plants. Appl Therm Eng 2016;103:274–81. doi:10.1016/j.applthermaleng.2016.04.116.

[36] Jin B, Zhao H, Zheng C. Thermoeconomic cost analysis of CO2 compression and purification unit in oxy-combustion power plants Bo. Energy 2015;83:416–30. doi:10.1016/j.energy.2015.02.039.

[37] Mathekga HI, Oboirien BO, North BC. A review of oxy-fuel combustion in fluidized bed reactors 2016:878–902. doi:10.1002/er.

[38] Lupion M, Alvarez I, Otero P, Kuivalainen R, Hotta A, Hack H. 30 MWth CIUDEN Oxy-CFB Boiler - First experiences. Energy Procedia 2013;37:6179–88. doi:10.1016/j.egypro.2013.06.547.

[39] Diego LF De, Obras-loscertales M De, Rufas A, Gayán P, Abad A, Adánez J. Pollutant emissions in a bubbling fluidized bed combustor working in oxy-fuel operating conditions : Effect of flue gas recirculation. Appl Energy 2013;102:860–7. doi:10.1016/j.apenergy.2012.08.053.

[40] El Hadri N, Quang DV, Goetheer EL V, Abu Zahra MRM. Aqueous amine solution characterization for post-combustion CO2 capture process. Appl Energy 2015;185:1433–49. doi:10.1016/j.apenergy.2016.03.043.

[41] Cohen SM, Webber ME, Rochelle GT. Utilizing Solar Thermal Energy for Post-Combustion

CO2 Capture. J Energy Power Eng 2011;3:195–208. doi:10.1115/ES2010-90147.

[42] Politecnico di Milano – Alstom UK (CAESAR project). European best practice guidelines for assessment of CO2 capture technologies. 2011.

[43] Aaron D, Tsouris C. Separation of CO2 from Flue Gas: A Review. Sep Sci Technol 2005;40:321–48. doi:10.1081/SS-200042244.

[44] Luis P. Use of monoethanolamine (MEA) for CO2 capture in a global scenario: Consequences and alternatives. Desalination 2016;380:93–9. doi:10.1016/j.desal.2015.08.004.

[45] Rey A, Gouedard C, Ledirac N, Cohen M, Dugay J, Vial J, et al. Amine degradation in CO2 capture. 2. New degradation products of MEA. Pyrazine and alkylpyrazines: Analysis, mechanism of formation and toxicity. Int J Greenh Gas Control 2013;19:576–83. doi:10.1016/j.ijggc.2013.10.018.

[46] Fytianos G, Ucar S, Grimstvedt A, Hyldbakk A, Svendsen HF, Knuutila HK. Corrosion and degradation in MEA based post-combustion CO2 capture. Int J Greenh Gas Control 2016;46:48–56. doi:10.1016/j.ijggc.2015.12.028.

[47] Dean CC, Blamey J, Florin NH, Al-Jeboori MJ, Fennell PS. The calcium looping cycle for CO2 capture from power generation, cement manufacture and hydrogen production. Chem Eng Res Des 2011;89:836–55. doi:10.1016/j.cherd.2010.10.013.

[48] Wang W, Ramkumar S, Wong D, Fan LS. Simulations and process analysis of the carbonation-calcination reaction process with intermediate hydration. Fuel 2012;92:94–106. doi:10.1016/j.fuel.2011.06.059.

[49] Manovic V, Anthony EJ. Competition of sulphation and carbonation reactions during looping cycles for CO2 capture by cao-based sorbents. J Phys Chem A 2010;114:3997–4002. doi:10.1021/jp910536w.

[50] Fennell PS, Davidson JF, Dennis JS, Hayhurst AN. Regeneration of sintered limestone sorbents for the sequestration of CO2 from combustion and other systems. J Energy Inst 2007;80:116–9. doi:10.1179/174602207X189175.

[51] Ylätalo J, Parkkinen J, Ritvanen J, Tynjälä T, Hyppänen T. Modeling of the oxy-combustion calciner in the post-combustion calcium looping process. Fuel 2013;113:770–9. doi:10.1016/j.fuel.2012.11.041.

[52] Arias B, Diego ME, Abanades JC, Lorenzo M, Diaz L, Martínez D, et al. Demonstration of steady state CO2 capture in a 1.7MWth calcium looping pilot. Int J Greenh Gas Control 2013;18:237–45. doi:10.1016/j.ijggc.2013.07.014.

[53] Dieter H, Bidwe AR, Varela-duelli G, Charitos A, Hawthorne C. Development of the calcium looping CO2 capture technology from lab to pilot scale at IFK , University of Stuttgart. Fuel 2014;127:23–37. doi:10.1016/j.fuel.2014.01.063.

[54] Valverde JM. A model on the CaO multicyclic conversion in the Ca-looping process. Chem Eng J 2013;228:1195–206. doi:10.1016/j.cej.2013.05.023.

[55] Valverde JM, Sanchez-Jimenez PE, Perez-Maqueda L. Calcium-looping for post-combustion CO2 capture. On the adverse effect of sorbent regeneration under CO2. Appl Energy 2014;126:161–71. doi:10.1016/j.apenergy.2014.03.081.

[56] Shimizu T, Hirama T, Hosoda H, Kitano K, Inagaki M, Tejima K. A twin fluid-bed reactor for removal of CO2 from combustion processes. Chem Eng Res Des 1999;77:62–8.

doi:10.1205/026387699525882.

[57] Abanades JC. The maximum capture efficiency of CO2 using a carbonation/calcination cycle of CaO/CaCO3. Chem Eng J 2002;90:303–6. doi:10.1016/S1385-8947(02)00126-2.

[58] Borgwardt RH. Calcium oxide sintering in atmospheres containing water and carbon dioxide. Ind Eng Chem Res 1989;28:493–500. doi:10.1021/ie00088a019.

[59] Ortiz C, Valverde JM, Chacartegui R, Benítez-Guerrero M, Perejón A, Romeo LM. The Oxy-CaL process: A novel CO2 capture system by integrating partial oxy-combustion with the Calcium-Looping process. Appl Energy 2017;196:1–17. doi:10.1016/j.apenergy.2017.03.120.

[60] Isabel Martínez, Gemma Grasa, Jarno Parkkinen, Tero Tynjälä, Timo Hyppänen, Ramón Murillo MCR. Review and research needs of Ca-Looping systems modelling for post-combustion CO2 capture applications. Int J Greenh Gas Control 2016;50:1–101. doi:10.1016/j.ijggc.2016.04.002.

[61] Ortiz C, Valverde JM, Chacartegui R. Energy Consumption for CO2 Capture by means of the Calcium Looping Process: A Comparative Analysis using Limestone, Dolomite, and Steel Slag. Energy Technol 2016:1–12. doi:10.1002/ente.201600390.

[62] Ströhle J, Junk M, Kremer J, Galloy A, Epple B. Carbonate looping experiments in a 1 MWth pilot plant and model validation. Fuel 2014;127:13–22. doi:10.1016/j.fuel.2013.12.043.

[63] Nataly Echevarria Huaman R, Xiu Jun T. Energy related CO2 emissions and the progress on CCS projects: A review. Renew Sustain Energy Rev 2014;31:368–85. doi:10.1016/j.rser.2013.12.002.

[64] Goto K, Yogo K, Higashii T. A review of efficiency penalty in a coal-fired power plant with post-combustion CO2 capture. Appl Energy 2013;111:710–20. doi:10.1016/j.apenergy.2013.05.020.

[65] Baker RW, Lokhandwala K. Natural Gas Processing with Membranes : An Overview 2008:2109–21.

[66] Merkel TC, Lin H, Wei X, Baker R. Power plant post-combustion carbon dioxide capture : An opportunity for membranes. J Memb Sci 2010;359:126–39. doi:10.1016/j.memsci.2009.10.041.

[67] Favre E. Membrane processes and postcombustion carbon dioxide capture : Challenges and prospects. Chem Eng J 2011;171:782–93. doi:10.1016/j.cej.2011.01.010.

[68] Chacartegui R, Monje B, Sánchez D, Becerra J a., Campanari S. Molten carbonate fuel cell: Towards negative emissions in wastewater treatment CHP plants. Int J Greenh Gas Control 2013;19:453–61. doi:10.1016/j.ijggc.2013.10.007.

[69] Discepoli G, Milewski J, Desideri U. Off-design operation of coal power plant integrated with natural gas fueled molten carbonate fuel cell as CO2 reducer. Int J Hydrogen Energy 2016;41:4773–83. doi:10.1016/j.ijhydene.2016.01.065.

[70] Milewski J, Bujalski W, Wołowicz M, Futyma K, Kucowski J, Bernat R. Experimental investigation of CO2 separation from lignite flue gases by 100 cm2 single Molten Carbonate Fuel Cell. Int J Hydrogen Energy 2014;39:1558–63. doi:10.1016/j.ijhydene.2013.08.144.

[71] Barelli L, Bidini G, Campanari S, Discepoli G, Spinelli M. Performance assessment of natural gas and biogas fueled molten carbonate fuel cells in carbon capture configuration. J Power Sources 2016;320:332–42. doi:10.1016/j.jpowsour.2016.04.071.

[72] Krieg JP, Winston AE. Dry carbonation process. United States Patent. US 06/487114 (US4459272 A), 1984.

[73] Falotico AJ. Dry carbonation of trona. PCT Application. PCT/US1992/006321 (WO1993/011070 A1), 1993.

[74] Nelson TO, Green DA, Box P, Gupta RP, Henningsen G, Turk BS. Carbon dioxide capture from flue gas using dry regenerable sorbents (Final Report). DOE Cooperative Agreement No. DE-FC26-00NT40923, RTI Project No. 0207887. 2009.

[75] Wang M, Lawal A, Stephenson P, Sidders J, Ramshaw C, Hill W, et al. Post-combustion CO2 capture with chemical absorption: A state-of-the-art review. Chem Eng Res Des 2011;89:1609–24. doi:10.1016/j.cherd.2010.11.005.

[76] Parvareh F, Sharma M, Qadir A, Milani D, Khalilpour R, Chiesa M, et al. Integration of solar energy in coal-fired power plants retrofitted with carbon capture: A review. Renew Sustain Energy Rev 2014;38:1029–44. doi:10.1016/j.rser.2014.07.032.

[77] Qadir A, Mokhtar M, Khalilpour R, Milani D, Vassallo A, Chiesa M, et al. Potential for solar-assisted post-combustion carbon capture in Australia. Appl Energy 2013;111:175–85. doi:10.1016/j.apenergy.2013.04.079.

[78] Liang Z, Fu K, Idem R, Tontiwachwuthikul P. Review on current advances, future challenges and consideration issues for post-combustion CO2 capture using amine-based absorbents. Chinese J Chem Eng 2016;24:278–88. doi:10.1016/j.cjche.2015.06.013.

[79] Mokhtar M, Ali MT, Khalilpour R, Abbas A, Shah N, Hajaj A Al, et al. Solar-assisted Post-combustion Carbon Capture feasibility study. Appl Energy 2012;92:668–76. doi:10.1016/j.apenergy.2011.07.032.

[80] Li H, Yan J, Campana PE. Feasibility of integrating solar energy into a power plant with amine-based chemical absorption for CO 2 capture. Int J Greenh Gas Control 2012;9:272–80. doi:10.1016/j.ijggc.2012.04.005.

[81] Wang F, Zhao J, Li H, Li H, Zhao L, Yan J. Experimental study of solar assisted post-combustion carbon capture. Energy Procedia 2015;75:2246–52. doi:10.1016/j.egypro.2015.07.401.

[82] Wang F, Zhao J, Li H, Deng S, Yan J. Preliminary experimental study of post-combustion carbon capture integrated with solar thermal collectors. Appl Energy 2016;185. doi:http://dx.doi.org/10.1016/j.apenergy.2016.02.040.

[83] Carapellucci R, Giordano L, Vaccarelli M. Analysis of CO2 post-combustion capture in coal-fired power plants integrated with renewable energies. Energy Procedia 2015;82:350–7. doi:10.1016/j.egypro.2015.11.801.

[84] Sharma M, Parvareh F, Abbas A. Highly integrated post-combustion carbon capture process in a coal-fired power plant with solar repowering. Int J Energy Res 2015;44:n/a-n/a. doi:10.1002/er.3361.

[85] Zhang X, Liu Y. Performance assessment of CO2 capture with calcination carbonation reaction process driven by coal and concentrated solar power. Appl Therm Eng 2014;70:13–24. doi:10.1016/j.applthermaleng.2014.04.072.

[86] Zhai R, Li C, Qi J, Yang Y. Thermodynamic analysis of CO2 capture by calcium looping process driven by coal and concentrated solar power. Energy Convers Manag 2016;117:251–63. doi:10.1016/j.enconman.2016.03.022.

[87] Tregambi C, Montagnaro F, Salatino P, Solimene R. A model of integrated calcium looping for CO2 capture and concentrated solar power. Sol Energy 2015;120:208–20. doi:10.1016/j.solener.2015.07.017.

[88] Heda PK, Dollimore D, Alexander KS, Chen D, Law E, Bicknell P. A method of assessing solid state reactivity illustrated by thermal decomposition experiments on sodium bicarbonate. Thermochim Acta 1995;255:255–72. doi:10.1016/0040-6031(94)02154-G.

[89] Otsubo Y, Yamaguchi K. Thermochemical Properties and Reaction Processes of Alkali Carbonate-Ferric Oxide Systems as Investigated by Means of Differential Thermal Method. I-II. I. Li2CO3-Fe2O3 System. Chem Soc Japan 1961;82:557–60. doi:http://doi.org/10.1246/nikkashi1948.82.5_557.

[90] Haynes HW. Thermodynamic solution model for trona brines. AIChE J 2003;49:1883–94. doi:10.1002/aic.690490724.

[91] Ciferno JP, Fout TE, Jones AP, Murphy JT. Capturing Carbon from Existing Coal-Fired Power Plants. Chem Eng Prog 2009;105:33–41.

[92] Ortiz C, Chacartegui R, Valverde JM, Becerra JA. A new integration model of the calcium looping technology into coal fired power plants for CO2 capture. Appl Energy 2016;169:408–20. doi:10.1016/j.apenergy.2016.02.050.

[93] Mills D. Pneumatic conveying design guide 2004:80.

[94] Chacartegui R, Vigna L, Becerra JA, Verda V. Analysis of two heat storage integrations for an Organic Rankine Cycle Parabolic trough solar power plant. Energy Convers Manag 2016;125:353–67. doi:10.1016/j.enconman.2016.03.067.

[95] Hoffschmidt PD-IB. Thermal Heat Storage Systems 2008.

[96] Winter, Sizmann V-H. Solar Power Plants – Fundamentals, Technology, Systems, Economics. Springer-Verlag; 1991.

[97] Bates J, Henry S. Carbon factor for wood fuels for the Supplier Obligation. Final report (AEA/ED01858010/Issue 2). 2009.

[98] J. Carlos Abanades *,†, G. Grasa ‡, M. Alonso †, N. Rodriguez †, E. J. Anthony § and, Romeo‖ LM. Cost Structure of a Postcombustion CO2 Capture System Using CaO 2007. doi:10.1021/ES070099A.

[99] European Coal Prices Slump to a Record Low - Bloomberg n.d.

[100] IRENA. Renewable Energy Technologies Cost Analysis Series: Concentrating Solar Power. vol. 1. 2012. doi:10.1016/B978-0-08-087872-0.00319-X.

[101] Jacobson M. Project economics for wood energy. Common forms of biomass. 2011.

[102] Junginger M, Goh CS, Faaij A. International Bioenergy Trade: History, status & outlook on securing sustainable bioenergy supply, demand and markets. Lecture No. Dordrecht: Springer Science & Business Media; 2014. doi:10.1007/978-94-007-6982-3.

[103] Lizana J, Ortiz C, Soltero VM, Chacartegui R. District Heating systems based on Low-Carbon Energy technologies in Mediterranean areas. Energy 2016. doi:10.1016/j.energy.2016.11.096.

Figures

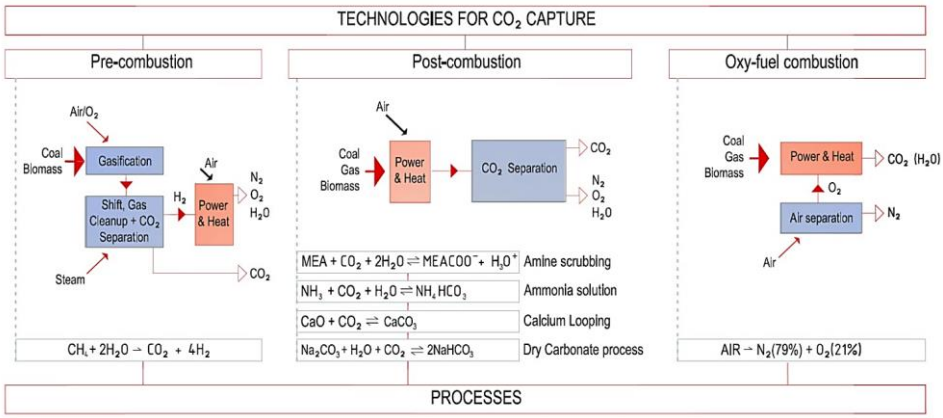

Figure 1: Overview of technologies for CO2 capture.

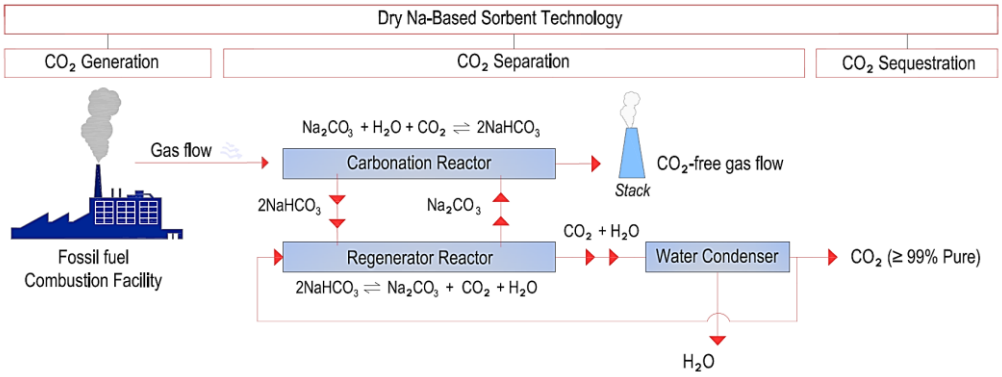

Figure 2: General scheme of the Dry Carbonate Process.

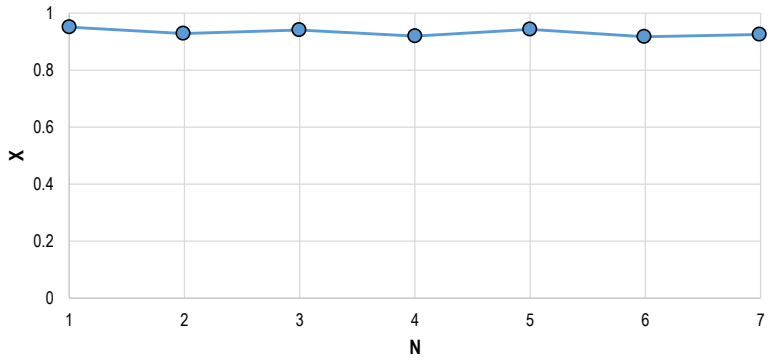

Figure 3: Na_2CO_3 conversion as a function of the cycle number (data extracted from [74]).

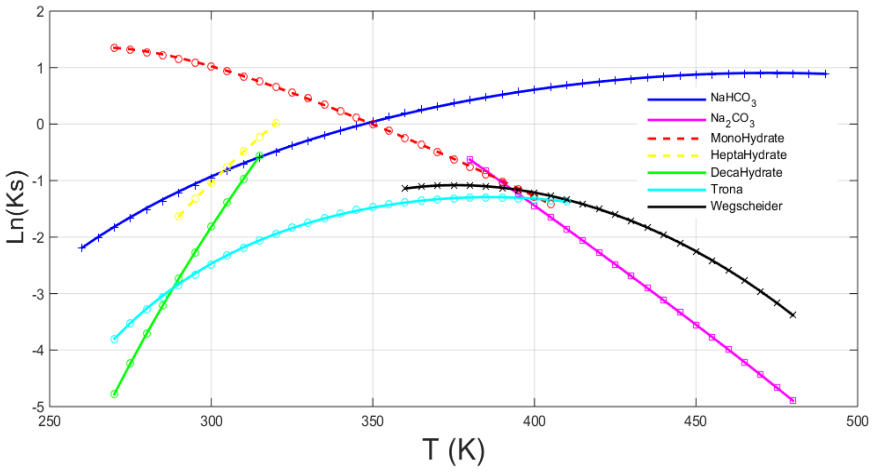

Figure 12: Ln(Ks) values for reactions involved in $NaHCO_3$ production from raw trona

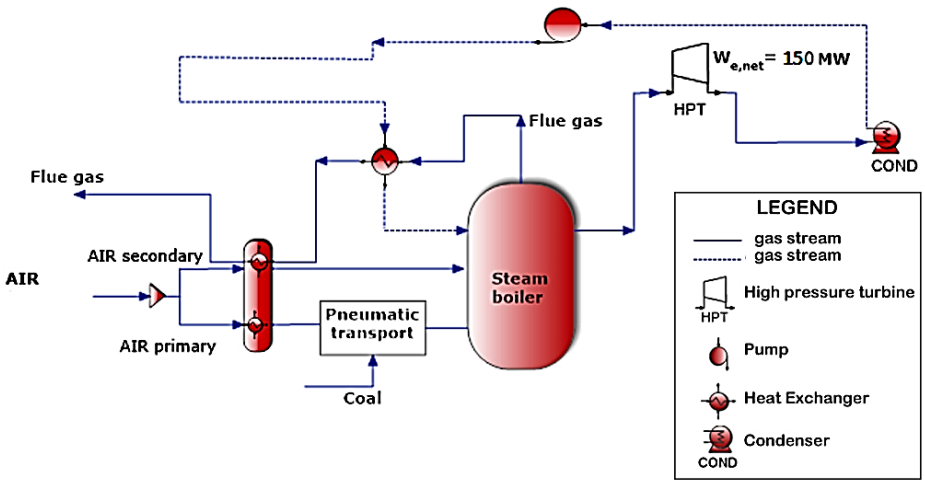

Figure 5: Reference coal fired power plant scheme used in the present work.

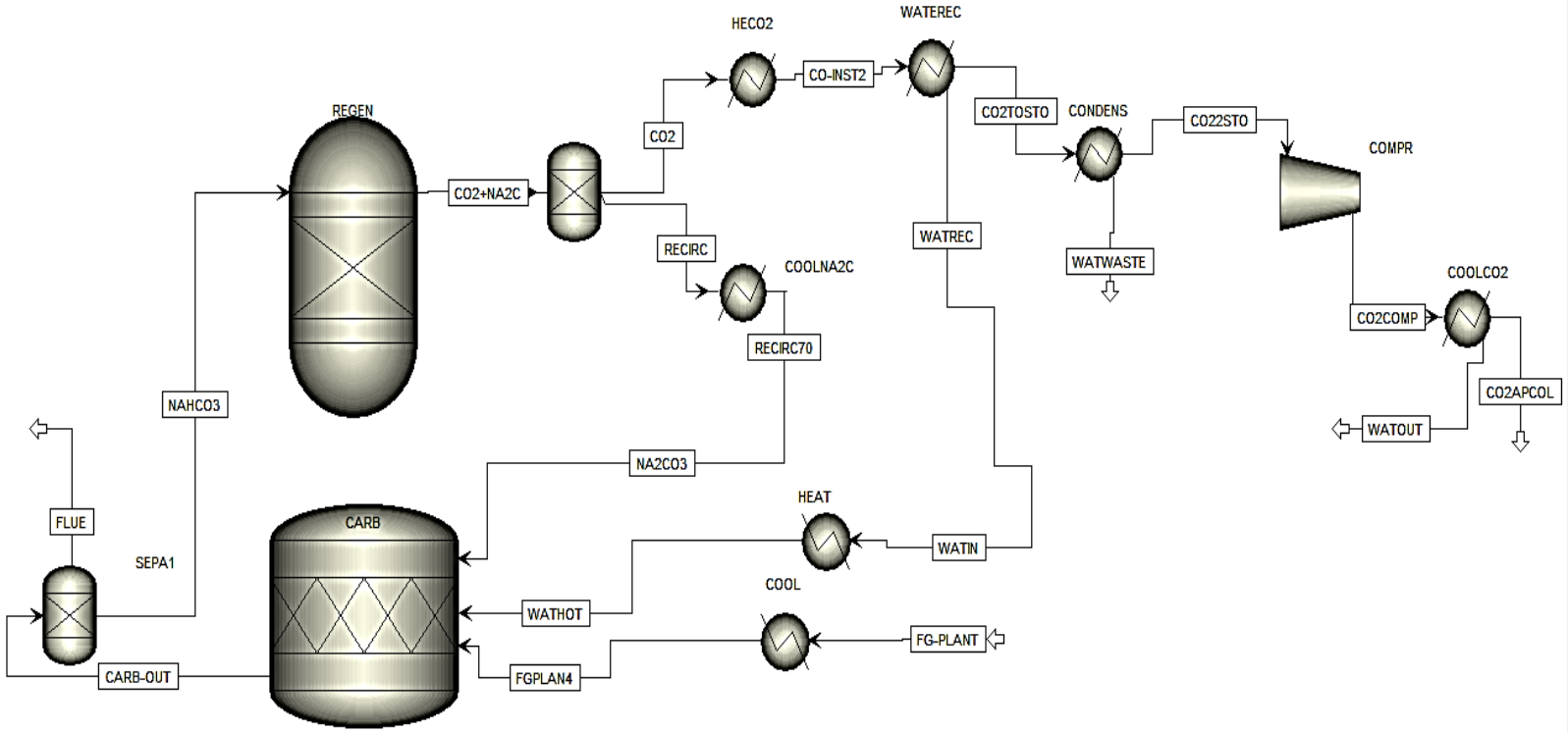

Figure 6: Dry Carbonate Process layout.

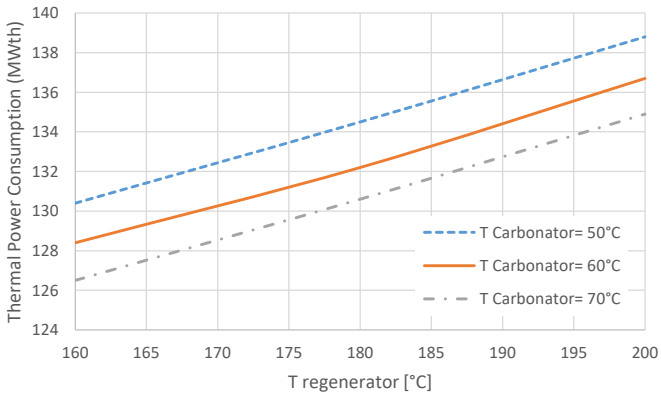

Figure 7: Thermal power required for different carbonator and regenerator temperatures.

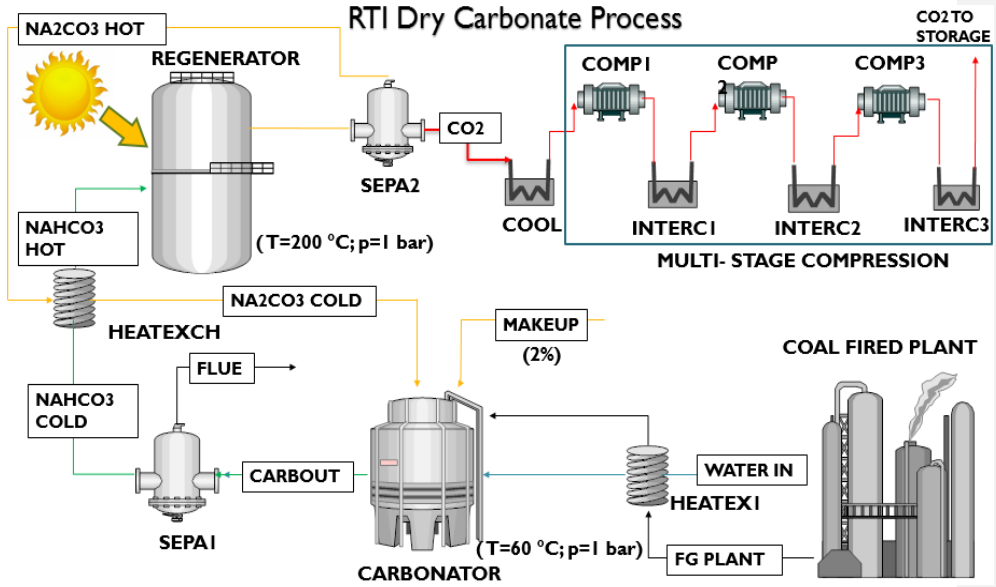

Acronyms (equipment and streams):

CARBONATOR: CO_2 capture reactor
CARBOUT: Final product from carbonator
CO_2: CO_2 recovered from the system
CO_2 TO STORAGE: CO_2 to the storage system (20 °C, 75 bar)
COAL FIRED PLANT: Coal fired plant for electricity production
COMP1: Compressor CO_2 (1-10 bar)
COMP2: Compressor CO_2 (10-25 bar)
COMP3: Compressor CO_2 (25-75 bar)
COOL: CO2 (20°C) intercooler
FGPLANT: Flue gas exits the coal fired plant
NA2CO3 COLD: Regenerated Na_2CO_3 (80°C)
NA2CO3 HOT: Regenerated Na_2CO_3 (200°C)
NAHCO3 COLD (fig.6): Solids exits the carbonator (60°C)
NAHCO3 HOT: Solids entering the regenerator (140°C)
HEATEX1 H_2O-flue gas heat exchanger
HEATEXCH: $NaHCO_3$-Na_2CO_3 heat exchanger
INTERC1: CO_2 (20°C) intercooler
INTERC2: CO_2 (20°C) intercooler
INTERC3: CO_2 (20°C) intercooler
MAKE UP: Sorbent Make up
REGENARATOR: Sorbent regenerator
SEPA1: Solid-gas separator
SEPA2: Solid-gas separator
WATER IN: Water to CO_2 capture reactor

Figure 8: Optimized plant configuration proposed in this work.

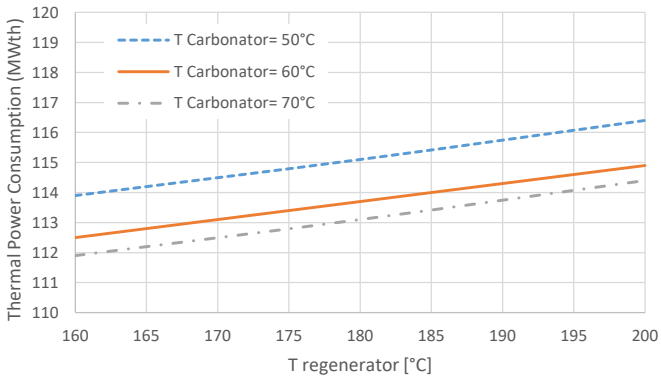

Figure 9: Power consumption for different operating conditions (including heat recovery).

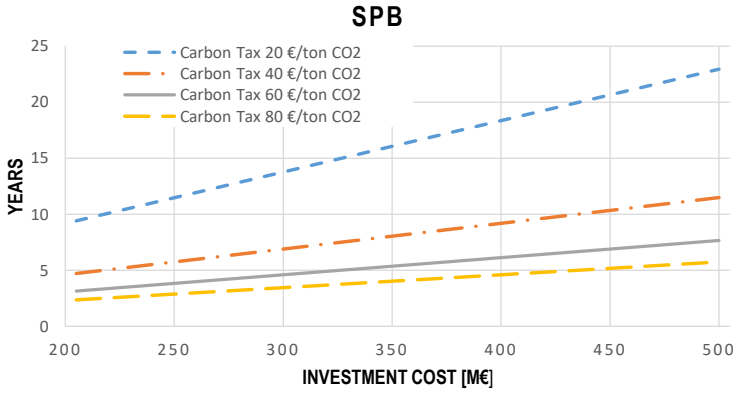

Figure 10: SPB curves according to the three scenarios as function of CFPP retrofitting capital costs.

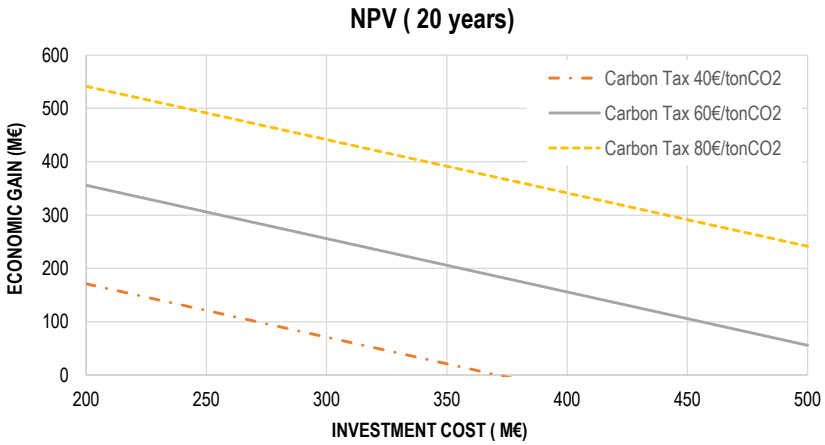

Figure 11: NPV for different carbon tax values and different investment costs.

Tables

Table 1: Reference data for a 150 MW_e coal fired plant (data scaled from [48]).

Item	Magnitude	Unit
Coal consumption	61	ton/hr
Air intake	692	ton/hr
Gross power introduced with fuel	447	MW_{th}
Net power supplied	397	MW_{th}
Net Power produced	150	MW_{el}
Net efficiency	33.5	%

Table 2: Flue gas flow for a 150 MW_e coal fired plant (data scaled from [48]).

Coal flue gas component	Mole Flow (kmol/hr)	Mass Flow (tons/hr)
N_2	17154.21	529.71
CO_2	3085.62	135.96
H_2O	1471.86	29.4
O_2	781.8	27.57
CO	140.7	3.93
NO	135.36	4.47
SO_2	37.53	2.64

Table 3: Carbonator and calciner working conditions.

	carbonator	calciner
Outlet temperature [°C]	60	140
Outlet pressure [bar]	1,01	1.01
Net heat duty [MW]	-101.240	122.480
Total feed stream CO2 flow [ton/h]	135.550	0
Total product stream CO2 flow [ton/h]	10.620	127.010
Net stream CO2 production [ton/h]	-124.930	127.010

Table 4: Calciner streams composition.

	CO_2+NA	$NAHCO_3H$
Temperature (°C)	140	60
Pressure (bar)	1.01	1.01
Mass flow (ton/hr)		
H_2O	50.28	1.44
CO_2	124	0
Na_2CO_3	323.25	442.7
$NaHCO_3$	0	11.39
Wegsheider's salt		44.39

Table 5: Power balance without heat recovery.

	Power production	Power consumption
CFFP	150 MW_{el}	447 MW_{th}
Decarbonator		122.5 MW_{th}
COMP		15 MW_{el}
Wsolid		2.37 MW_{el}
Net Power	132.53 MW_{el}	
Total heat requirement		569.5 MW_{th}

Table 6: CO_2 compression power

	two-stage compression		three-stage compression	
Component	Exhaust Pressure (bar)	Power (MW)	Exhaust Pressure (bar)	Power (MW)
COMP1	9	6.29	4.2	3.78
COMP2	75	6.02	17.6	3.78
COMP3	-	-	75	3.6
Global W_{comp}		**12.31**		**11.16**

Table 7: Global plant energy balance.

	Power production	Power consumption
CFFP	150 MWel	447 MWth
Decarbonator		114.9 MWth
COMP		11.16 MWel
Wsolid		2.47 MWel
Net Power	136.37 MWel	
Total heat		561.9 MWth

Table 8: Efficiency values for different sorbent conversion factors (X).

X	Na_2CO_3 flow (kmol/hr)	Calciner (MW_{th})	Carbonator (MW_{th})	W_{solid} (MW_{el})	Efficiency (%)
0.4	84.5	119.5	-104	4.6	23.2
0.75	42.93	114.9	-101	2.47	24.2
0.95	32.86	111	-98	1.89	24.37

Table 9: Main properties of materials to store energy in the form of sensible heat [95,96]

	Temperature (°C) Cold	Hot	Average density (kg/m^3)	Average heat conductivity (W/(mK))	Average heat capacity (kJ/(kgK))	Thermal diffusivity (m^2/s)	Volume specific heat capacity (kWh_{th}/m^3)	Volume (m^3)
Solid storage media								
Sand-rock-mineral oil	200	300	1700	1.0	1.30	4.5×10-7	60	22460.1
Reinforced concrete	200	400	2200	1.5	0.85	8.0×10-7	100	13271.9
Cast iron	200	400	7200	37.0	0.56	9.2×10-6	160	6155.4
Liquid storage media								
Mineral oil	200	300	770	0.12	2.6	6.0×10-8	55	24793.6
Synthetic oil	250	350	900	0.11	2.3	5.3×10-8	57	23979.1
Silicone oil	300	400	900	0.10	2.1	5.3×10-8	52	Out of range
Nitrite salts	250	450	1825	0.57	1.5	2.1×10-7	152	Out of range

Table 10: Properties of different typologies of wood chips

Wood chips	H_i[MJ/kg]	ρ[kg/m^3]	H_i[MJ/ m^3]
Chestnut	10,53	580	6106,24
Beech	13,45	750	10084,95
Spruce	7,90	450	3556,98
Larch	11,60	660	7654,88
Average	10,87	610	6630,29

Table 11: CO_2 emission data for different scenarios.

	REFERENCE PLANT	DRY CARBONATE (P)	DRY CARBONATE (BE)	DRY CARBONATE (O)
Power (MWel)	150	150	150	150
CCS Power consumption (MWel)	-	25	13.63	13
Regenerator Heat requirement (MWth)	-	119	114.9	111
Net power (MWel)	150	125	136.37	137
CO_2 Emissions (ton/hr)	136	10.7	10.7	10.7
CO_2 Emissions (kmol/hr)	3080	243.2	243.2	243.2
CO_2 Avoided Emissions (kton/year)		1089	1089	1089
CO_2 Emissions (tons/ MWhel/hr)	0.9	0.085	0.078	0.078

Table 12: SPECCA Analysis for different scenarios.

Item	Scen.P	Scen. BE	Scen. O
Net Power Production (MW)	125	136,37	137
$CO_{2\ CCS}$ (ton/hr)	10,7	10,7	10,7
E_{CCS} (kg_{CO2}/kWh_{el})	85.60	78.46	78.10
η_{CCS}	0.232	0.242	0.244
SPECCA (MJ/kg_{CO2})	5.86	5.03	4.90
η_{CCS_ECO}	0.279	0.305	0.306
$SPECCA_{\_ECO}$(MJ/kg_{CO2})	2.65	1.29	1.24

Table 13: COE for different scenarios.

Item	Item	Units	Scen. P	Scen. BE	Scen. O
Fuel Cost [99]	FC	€/kWh	0.03	0.023	0.02
Capital Cost	TCR	€/kWe	1200	1100	1000
Fixed Charge Factor [99]	FCF	$year^{-1}$	0.15	0.1	0.075
Variable Cost	VOM	€/kWe	0.006	0.006	0.006
COE_{ref}		€/kWh	0.116	0.087	0.074

Table 14: COE for CCS system (as function of Solar Capital Costs).

Item	Item	Units	Scen. PE	Scen. BE	Scen. O
Net Power Production		MW_e	125	136.37	137
η_{el}			27.9	29.9	30.2
η_{system}		%	22.1	24.2	24.37
Dry Carb. Capital cost [6]	TCR	M€/MW	0.32	0.223	0.148
Solar Capital Cost [100]	TCR	M€/MW	1.5		
COECCS		€/kWh	0.165	0.115	0.095
AC		€/ton_{CO2}	60.416	34.245	25.421
Solar Capital Cost [100]	TCR	M€/MW	2		
COECCS		€/kWh	0.174	0.121	0.099
AC		€/ton_{CO2}	64.223	41.188	30.629
Solar Capital Cost [100]	TCR	M€/MW	2.5		
COECCS		€/kWh	0.182	0.127	0.103
AC		€/ton_{CO2}	73.736	48.132	35.837
Solar Capital Cost [100]	TCR	M€/MW	3		
COECCS		€/kWh	0.191	0.132	0.108
AC		€/ton_{CO2}	83.249	55.076	41.045
Solar Capital Cost [100]	TCR	M€/MW	3.5		
COECCS		€/kWh	0.199	0.138	0.112
AC		€/ton_{CO2}	92.762	62.020	46.253

Table 15: ΔCOE (€/kWh$_{el}$) for different costs of solar thermal field.

Solar Thermal cost (€/kW$_t$)	Scen. P	Scen. BE	Scen. O
1500	0.0492	0.0281	0.0209
2000	0.0578	0.0339	0.0252
2500	0.0664	0.0396	0.0295
3000	0.0749	0.0453	0.0337
3500	0.0835	0.0510	0.0380

Table 16: Total CFPP retrofitting investment cost calculated by considering several CSP plant prices.

Solar Thermal Cost 1.5 M€/MW				
	Units	Scen. P	Scen. BE	Scen. O
ESOLAR	M€	179.25	172.35	166.5
EDRY	M€	40	30	20
EO&M	M€	21.92	20.23	18.65
ETOT	M€	241.17	222.58	205.15
Solar Thermal Cost 2 M€/MW				
	Units	Scen. P	Scen. BE	Scen. O
ESOLAR	M€	239	229.8	222
EDRY	M€	40	30	20
EO&M	M€	27.9	25.98	24.2
ETOT	M€	306.9	285.78	266.2
Solar Thermal Cost 2.5 M€/MW				
	Units	Scen. P	Scen. BE	Scen. O
ESOLAR	M€	298.75	287.25	277.5
EDRY	M€	40	30	20
EO&M	M€	33.87	31.725	29.75
ETOT	M€	372.62	348.975	327.25
Solar Thermal Cost 3 M€/MW				
	Units	Scen. P	Scen. BE	Scen. O
ESOLAR	M€	358.5	344.7	333
EDRY	M€	40	30	20
EO&M	M€	39.85	37.47	35.3
ETOT	M€	438.35	412.17	388.3
Solar Thermal Cost 3.5 M€/MW				
	Units	Scen. P	Scen. BE	Scen. O
ESOLAR	M€	418.25	402.15	388.5
EDRY	M€	40	30	20
EO&M	M€	45.82	43.21	40.85
ETOT	M€	504.07	475.36	449.35

Table 17: Required increment of electricity sale price for maintaining a fixed value of IRR=0.1

	Total Investment Cost (M€)	E_{incr} (M€/year)	Δ Electricity price (c€/kWh)
Without Carbon Tax	200	23.5	1.967
	300	35.2	2.947
	400	47	3.934
	500	58.8	4.922
Carbon Tax 20 €/tonCO2	200	0	0
	300	11.6	0.971
	400	23.4	1.959
	500	35.2	2.947
Carbon Tax 40€/tonCO2	200	0	0
	300	0	0
	400	0	0
	500	11.5	0.963